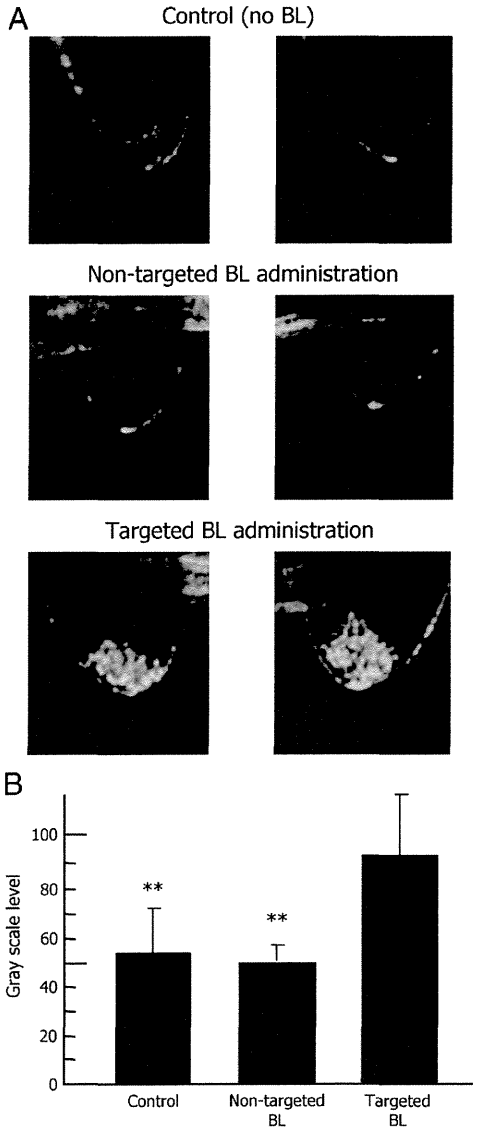


**Fig. 1.** Ultrasonic thrombus imaging is apparently enhanced by targeted BL *in vitro* when compared to control and non-targeted BL (A). Video intensity levels of the thrombi in the targeted BL group were significantly higher than in the control and non-targeted BL groups (B). BL: bubble liposomes.

mean pixel gray-scale level of the thrombus at 1 min ($25.5 \pm 4.8$ vs. $26.4 \pm 5.3$, $p = 0.3329$, $n = 10$) (Fig. 3B and C).

## 4. Discussion

In our *in vitro* and *in vivo* studies, we confirmed that ultrasound imaging of thrombi is markedly enhanced by targeted BL, even via intravenous administration using a conventional diagnostic ultrasound machine. This is also the first study to show the feasibility of perfluorocarbon gas-containing liposomes, rather than a phospholipid mono-layer, as a targeted ultrasound contrast agent, in addition to a carrier for gene delivery [11–13].

In clinical settings, various ultrasound contrast agents with lipid-based or non-lipid-based shells are commercially available for diagnostic use. These agents are prepared to enhance blood flow or tissue perfusion. Some of these agents are capable of passively imaging inflammation using the inherent chemical properties of the shell components [22]. However, they have no specific ligands on their surface for actively targeting pathophysiological molecules.

Lanza et al. first reported a fibrin-targeting ultrasonic contrast agent. They used lipid-encapsulated, nongaseous perfluorocarbon emulsion and an antifibrin monoclonal antibody as a targeting ligand, incorporating avidin-biotin triphasic interaction steps to demonstrate excellent thrombus enhancement [4]. However, this technique has limited applications in humans due to the complexity of targeting interactions and immunogenicity of avidin [23]. Unger et al. developed thrombus-targeting perfluorocarbon gas-containing microbubbles with lipid mono-layer shells incorporating small peptides as ligands for activated platelets [5–7]. This agent was able to enhance ultrasonic thrombus imaging both *in vitro* and *in vivo* during continuous intravenous infusion. Demos and Hamilton reported thrombus-targeting nongaseous echogenic immuno-liposomes, which enhanced ultrasonic imaging of both intravascular and intracardiac thrombi [8,9]. In this study, anti-fibrinogen antibody was used as the targeting ligand, which may cause systemic adverse effects due to secondary immunoreactions. Alonso et al. developed abciximab, an antibody fragment specific for the glycoprotein IIb/IIIa receptor, bearing immunobubbles with phospholipid mono-layer shells. These immunobubbles improved visualization of human clots both *in vitro* and in an *in vivo* model of acute arterial thrombotic occlusion [10].

Targeted BL shows some advantages over these previously reported thrombus-targeting ultrasound contrast agents [4–10]. We used liposomes as a basic structure, as a lipid bi-layer shell increases the stability of BL and works as a barrier against gas diffusion [12], and the liposomal surface can be modified for the conjugation of various targeted ligands, as well as for achieving longer circulation times. Polyethylene glycol was attached to the surface lipid layer in order to

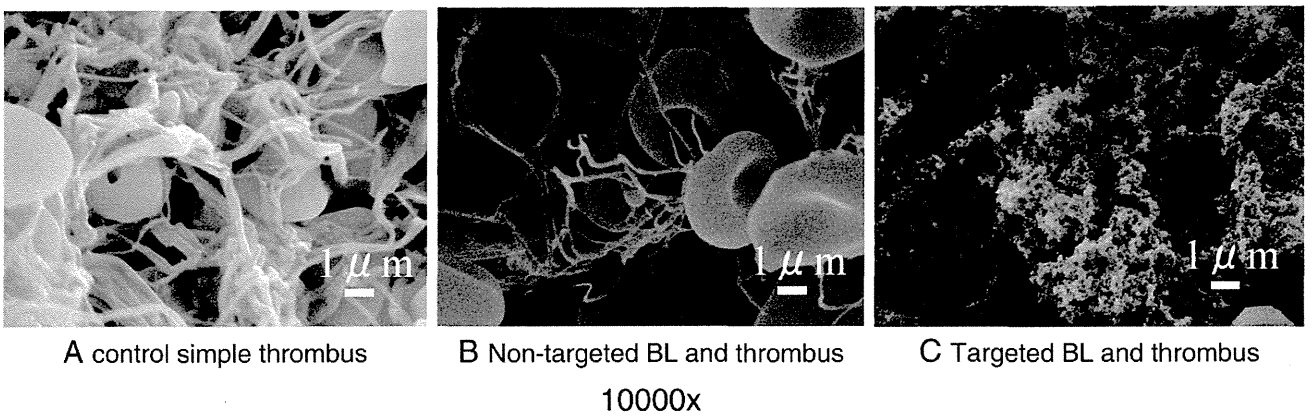


**Fig. 2.** Scanning electron microscopy revealed large amounts of BL attached to the thrombi in the targeted BL group (C), which were not observed in the non-targeted BL (B) and control groups (A). BL: bubble liposomes.

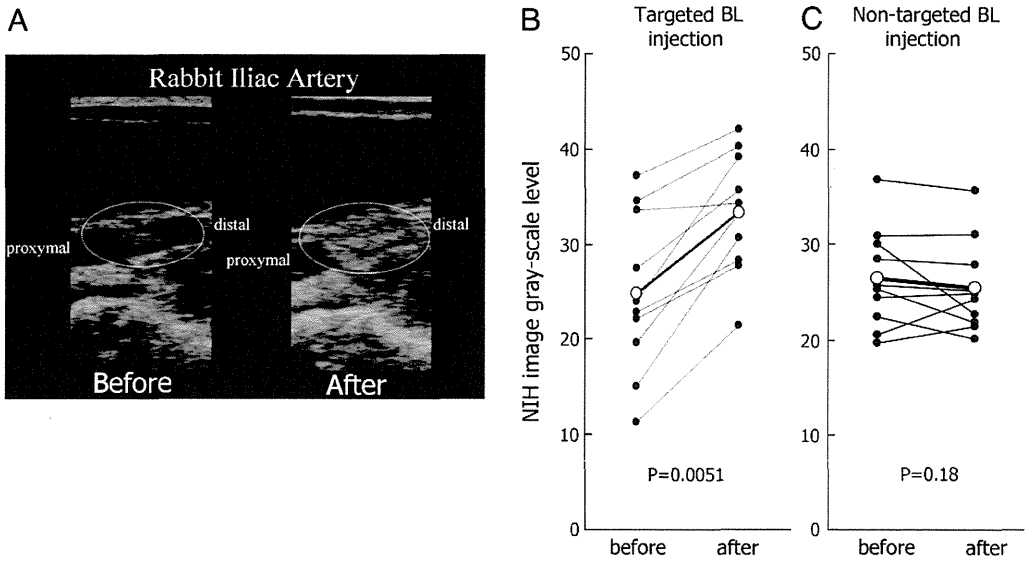


**Fig. 3.** Ultrasound image of *in vivo* thrombi is significantly enhanced after administration of targeted BL via an ear vein. (A) NIH image quantitative analysis shows significant increases on *in vivo* thrombus echo intensity by intravenous administration of targeted BL; (B) however, similar changes are not seen after administration of non-targeted BL (C). BL: bubble liposomes.

increase hydrophilicity, thereby offering a stealth effect with respect to reticulo-endothelial capture and allowing longer circulation times [24,25]. Moreover, a BL size of less than a micron (nano-size) permits deeper penetration into thrombi.

The targets of ultrasonic thrombus imaging have been fibrin [4,8,9] or activated platelets [5–7,10]. Fibrin is typically present in all types of thrombi (arterial and venous, acute and chronic). In contrast, activated platelets are found in fresh thrombi in cases of acute coronary syndrome and stroke. The RGD sequence-containing peptide is a ligand for the activated platelet membrane glycoprotein IIb/IIIa complex. The RGD peptide is chemically stable and easily conjugated to the lipid surface layer, as it is composed of a small number of amino acids and binds strongly to phospholipids via a thio-ether bond without the need for complex chemical synthesis [14,15]. In contrast to antibodies, peptides are generally smaller in size and simpler in structure, resulting in less immunoreactivity [26,27]. Among the various types of RGD peptides, we used an octapeptide (CGGGRGDF) in this study. The initial C of this peptide was used for coupling and GGG served as an "arm" to distance the active RGD binding site from thiol-coupling to maleimide on the liposomal surface [17]. Moreover, this peptide has been reported to be a potent inhibitor of platelet agglutination through the glycoprotein IIb/IIIa receptor, and to be uniquely sensitive to the activation state of this receptor, even after incorporation into liposomes with polyethylene glycol modification [14,17].

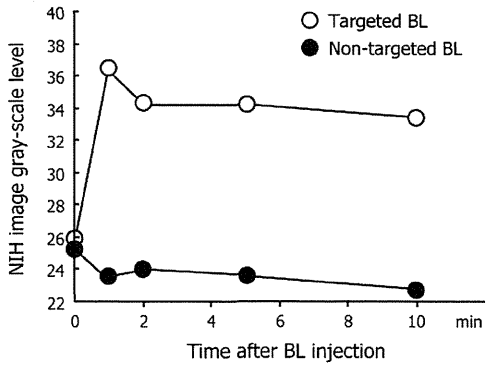


**Fig. 4.** Representative time-intensity curves of thrombi video intensity immediately before and after targeted and non-targeted BL injection measured using NIH image. Targeted BL significantly increased the mean pixel gray-scale level of the thrombus from 1 to 10 min after injection; however, no significant increases were observed after non-targeted BL injection. BL: bubble liposomes.

The mean diameter of this targeted BL was 0.18 μm. Theoretically, a single BL of this size is out of the diagnostic range of conventional ultrasound imaging. However, BL are apparently echogenic and are clearly visualized with high echo-intensity using conventional ultrasound machines [11]. As shown in the scanning electron microscopic section of this study, the targeted BL accumulated deep within the inner portions of the thrombi, as well as on the surface. This may have been due to the apparently smaller size of BL relative to the space between fibrin nets, and could also explain the strong enhancement on ultrasonic imaging both *in vitro* and *in vivo*. Non-targeted BL were unable to enhance thrombus imaging, probably due to the insufficient amount of BL passively retained around and within the thrombi required for echogenicity.

Liposomes are usually considered nontoxic unless administered at very high doses [28]. Liposomal drugs are already commercially available and are safely used in humans [29–31]. Polyethylene glycol is also considered nontoxic and is excreted unmetabolized in the urine [32]. The RGD peptide is an octapeptide and is considered to be non-toxic and non-immunogenic [26,27]. Perfluoropropane is an inert gas, used as a constituent of commercially available echo contrast agents such as Optison and Definity [33], and is exhaled from the lungs [34]. Therefore, this echo contrast agent is generally considered nontoxic, although safety in humans remains to be demonstrated. Other potential barriers for clinical use are related to the specificity of the RGD peptide. This ligand is highly specific to activated platelet glycoprotein IIb/IIIa receptor [14,17]. However, the specificity is limited and this ligand may also bind to sites of angiogenesis, inflammation, osteoporosis and cancer [35]. In contrast, the relatively high specificity of this ligand to activated platelets may prevent the attachment of the targeted BL to organized chronic thrombi, although this hypothesis was not examined in the present experiment. Therefore, this agent may only enhance fresh thrombi on imaging and may provide a unique opportunity to distinguish fresh thrombi from old organized thrombi. Another limitation of this study is that we did not use the harmonic imaging technique, which is considered to improve ultrasound image quality, particularly when used with echo contrast agents. With the use of harmonic imaging, more distinct enhancement of thrombi can be expected in larger animals or humans.

In conclusion, perfluorocarbon gas-containing liposomal bubbles with RGD peptides are a novel echo contrast agent that can markedly enhance fresh thrombi on ultrasonic imaging *in vitro* and *in vivo*, and may be useful for noninvasive diagnosis of acute thrombotic vessel occlusion.

## Acknowledgements

This study was supported in part by a Grant-in-Aid for Scientific Research (B) (16300176) from the Japan Society for the Promotion of Science and a Japan Heart Foundation Research Grant.

The authors of this manuscript have certified that they comply with the Principles of Ethical Publishing in the International Journal of Cardiology [36].

## References

[1] Masses, tumors, and source of embolus. In: Feigenbaum H, Armstrong WF, Ryan T, editors. Feigenbaum's echocardiography. 6th ed. Philadelphia, PA: Lippincott Williams & Wilkins; 2005. p. 701–34.
[2] Rose SC, Zwiebel WJ, Murdock LE, et al. Insensitivity of color Doppler flow imaging for detection of acute calf deep venous thrombosis in asymptomatic postoperative patients. J Vasc Interv Radiol 1993;4:111–7.
[3] Popma JJ. Coronary arteriography and intravascular imaging. In: Libby P, Bonow RO, Mann DL, Zipes DP, editors. Braunwald's heart disease: a textbook of cardiovascular medicine. 8th ed. Philadelphia, PA: Saunders Elsevier; 2008. p. 495–6.
[4] Lanza GM, Wallace KD, Scott MJ, et al. A novel site-targeted ultrasonic contrast agent with broad biomedical application. Circulation 1996;94:3334–40.
[5] Unger EC, McCreery TP, Sweitzer RH, Shen D, Wu G. In vitro studies of a new thrombus-specific ultrasound contrast agent. Am J Cardiol 1998;81:58G–61G.
[6] Wu Y, Unger EC, McCreery TP, et al. Binding and lysing of blood clots using MRX-408. Invest Radiol 1998;33:880–5.
[7] Takeuchi M, Ogunyankin K, Pandian NG, et al. Enhanced visualization of intravascular and left atrial appendage thrombus with the use of a thrombus-targeting ultrasonographic contrast agent (MRX-408A1): in vivo experimental echocardiographic studies. J Am Soc Echocardiogr 1999;12:1015–21.
[8] Demos SM, Alkan-Onyuksel H, Kane BJ, et al. In vivo targeting of acoustically reflective liposomes for intravascular and transvascular ultrasonic enhancement. J Am Coll Cardiol 1999;33:867–75.
[9] Hamilton A, Huang SL, Warnick D, et al. Left ventricular thrombus enhancement after intravenous injection of echogenic immunoliposomes: studies in a new experimental model. Circulation 2002;105:2772–8.
[10] Alonso A, Della Martina A, Stroick M, et al. Molecular imaging of human thrombus with novel abciximab immunobubbles and ultrasound. Stroke 2007;38:1508–14.
[11] Suzuki R, Takizawa T, Negishi Y, et al. Gene delivery by combination of novel liposomal bubbles with perfluoropropane and ultrasound. J Control Release 2007;117:130–6.
[12] Suzuki R, Takizawa T, Negishi Y, et al. Tumor specific ultrasound enhanced gene transfer in vivo with novel liposomal bubbles. J Control Release 2008;125:137–44.
[13] Suzuki R, Takizawa T, Negishi Y, Utoguchi N, Maruyama K. Effective gene delivery with liposomal bubbles and ultrasound as novel non-viral system. J Drug Target 2007;15:531–7.
[14] Gyongyossy-Issa MIC, Muller W, Devine DV. The covalent coupling of Arg-Gly-Asp-containing peptides to liposomes: purification and biochemical function of the lipopeptide. Arch Biochem Biophys 1998;353:101–8.
[15] Nishiya T, Sloan S. Interaction of RGD liposomes with platelets. Biochem Biophys Res Commun 1996;224:242–5.
[16] Szoka Jr F, Papahadjopolus D. Procedure for preparation of liposomes with large internal aqueous space and high capture by reverse-phase evaporation. Proc Natl Sci U S A 1978;75:4194–8.
[17] Beer JH, Springer KT, Coller BS. Immobilized Arg-Gly-Asp (RGD) peptides of varying lengths as structural probes of the platelet glycoprotein IIb/IIIa receptor. Blood 1992;79:117–28.
[18] NIH image home page. http://rsb.info.nih.gov/nih-image/ Accessed January 29, 2010.
[19] Glauert AM, Lewis PR. Biological specimen preparation for transmission electron microscopy. In: Glauert AM, editor. Practical methods in electron microscopy Volume 17. London, UK: Portland Press; 1998.
[20] Steffen W, Fishbein MC, Luo H, et al. High intensity, low frequency catheter-delivered ultrasound dissolution of occlusive coronary artery thrombi: an in vitro and in vivo study. J Am Coll Cardiol 1994;24:1571–9.
[21] Nishioka T, Luo H, Fishbein MC, et al. Dissolution of thrombotic arterial occlusion by high intensity, low frequency ultrasound and dodecafluoropentane emulsion: an in vitro and in vivo study. J Am Coll Cardiol 1997;30:561–8.
[22] Lindner JR. Microbubbles in medical imaging: current applications and future directions. Nature Rev Drug Discov 2004;3:527–32.
[23] Lanza GM, Wickline SA. Targeted ultrasonic contrast agents for molecular imaging and therapy. Curr Probl Cardiol 2003;28:625–53.
[24] Klibanov AL, Maruyama K, Torchilin VP, Huang L. Amphipathic polyethyleneglycols effectively prolong the circulation time of liposomes. FEBS Lett 1990;268:235–7.
[25] Maruyama K, Yuda T, Okamoto A, Kojima S, Suginaka A, Iwatsuru M. Prolonged circulation time in vivo of large unilamellar liposomes composed of distearoyl phosphatidylcholine and cholesterol containing amphipathic poly(ethylene glycol). Biochim Biophys Acta 1992;1128:44–9.
[26] Lee TY, Lin CT, Kuo SY, Chang DK, Wu HC. Peptide-mediated targeting to tumor blood vessels of lung cancer for drug delivery. Cancer Res 2007;67:10958–65.
[27] Chang DK, Lin CT, Wu CH, Wu HC. A novel peptide enhances therapeutic efficacy of liposomal anticancer drugs in mice models of human lung cancer. PLoS ONE 2009;4:e4171.
[28] Storm G, Oussoren C, Peelers PAM, Barenholz Y. Tolerability of liposomes *in vivo*. In: Gregoriadis G, editor. Liposome technology. Boca Raton, FL: CRC Press, Inc.; 1993. p. 345–83.
[29] Davidson RN, Croft SL, Scott A, Maini M, Moody AH, Bryceson AD. Liposomal amphotericin B in drug-resistant visceral leishmaniasis. Lancet 1991;337:1061–2.
[30] Guaglianone P, Chan K, DelaFlor-Weiss E, et al. Phase I and pharmacologic study of liposomal daunorubicin (DaunoXome). Invest New Drugs 1994;12:103–10.
[31] Gabizon A, Peretz T, Sulkes A, et al. Systemic administration of doxorubicin-containing liposomes in cancer patients: a phase I study. Eur J Cancer Clin Oncol 1989;25:1795–803.
[32] Carpenter CP, Woodside MD, Kinkead ER, King JM, Sullivan LJ. Response of dogs to repeated intravenous injection of polyethylene glycol 4000 with notes on excretion and sensitization. Toxicol Appl Pharmacol 1971;18:35–40.
[33] Wei K, Mulvagh SL, Carson L, et al. The safety of Definity and Optison for ultrasound image enhancement: a retrospective analysis of 78, 383 administered contrast doses. J Am Soc Echocardiogr 2008;11:1202–6.
[34] Hutter JC, Luu HM, Mehlhaff PM, Killam AL, Dittrich HC. Physiologically based pharmacokinetic model for fluorocarbon elimination after the administration of an octafluoropropane-albumin microsphere sonographic contrast agent. J Ultrasound Med 1999;18:1–11.
[35] Meyer A, Auernheimer J, Modlinger A, Kessler H. Targeting RGD recognizing integrins: drug development, biomaterial research, tumor imaging and targeting. Curr Pharm Des 2006;12:2723–47.
[36] Coats AJ. Ethical authorship and publishing. Int J Cardiol 2009;131:149–50.

ELSEVIER



# Pathological changes in tight junctions and potential applications into therapies

**Azusa Takahashi, Masuo Kondoh, Hidehiko Suzuki, Akihiro Watari and Kiyohito Yagi**

Laboratory of Bio-Functional Molecular Chemistry, Graduate School of Pharmaceutical Sciences, Osaka University, Osaka 565-0871, Japan

**Epithelial cells are pivotal in the separation of the body from the outside environment. Orally administered drugs must pass across epithelial cell sheets, and most pathological organisms invade the body through epithelial cells. Tight junctions (TJs) are sealing complexes between adjacent epithelial cells. Modulation of TJ components is a potent strategy for increasing absorption. Inflammation often causes disruption of the TJ barrier. Molecular imaging technology has enabled elucidation of the dynamics of TJs. Molecular pathological analysis has shown the relationship between TJ components and molecular pathological conditions. In this article, we discuss TJ-targeted drug development over the past 2 years.**

During evolution from single-celled to multi-celled organisms, a compartment system developed to separate the inside of the body from the outside environment. This compartment system is made up of epithelial and endothelial cell sheets. Sealing of the intercellular space between individual epithelial or endothelial cells is crucial for compartmentalization.

Tight junctions (TJs) are the apical-most component of intercellular seals. TJs are directly involved both in the sealing of paracellular spaces and in two major functions of membranes: the barrier function and the fence function [1,2]. The barrier function is the first line of defense against pathogenic microorganisms and xenobiotics, and the fence function regulates cellular polarity. Deregulation of these functions is often observed in infectious diseases, inflammation and carcinogenesis.

Freeze-fracture electron microscopy analysis has shown that TJs are a set of continuous and anastomosing strands [3]. A series of analyses revealed that TJ-seals contain integral membrane proteins, such as occludin, claudins and junctional adhesion molecules (Fig. 1) [4–6]. The claudin protein family comprises 27 members and the junctional adhesion molecule (JAM) family comprises 3 members [4,7]. A tricellular junction-sealing component, tricellulin, has also been identified in epithelial cell sheets [8]. Occludin and tricellulin contain the tetra-spanning and other related proteins for vesicle trafficking and membrane line (MARVEL) domain. Occludin and tricellulin are members of the MARVEL protein family [9]. MarvelD3, another member of the MARVEL protein family, has been identified as a component of TJs [10]. The intracellular constituents of TJs, ZO-1 and ZO-2, determine where the claudin-based strands are formed [11]. Lipolysis-stimulated lipoprotein receptors define where tricellular junctions are formed [12]. These biochemical components of TJ-seals were all clarified within a single decade [5,6,13]. Our understanding of TJ-components has provided us with a new perspective on drug delivery and drug discovery for infectious diseases, inflammations and cancers [14–16].

There have been two main progressions in our understanding of the biology of TJs within the past 2 years: mucosal barrier homeostasis and TJ barrier homeostasis. Proof-of-concepts for TJ-targeted drug delivery have been demonstrated. In this article, we discuss recent topics in TJ biology and TJ-targeted therapy.

## Biology of the epithelial barrier

### *Tight junctions*

Epithelium is central to the construction of multicellular animals. More than 60% of the cell types in the vertebrate body are epithelial cells. Epithelia enclose and partition the animal body, line all of its surfaces and cavities, and create internal compartments. Epithelial cells are structurally polarized into a basal side that is anchored to other tissue, and an apical side that is

*Corresponding author:*. Kondoh, M. (masuo@phs.osaka-u.ac.jp)

1359-6446/06/$ - see front matter © 2012 Published by Elsevier Ltd. doi:10.1016/j.drudis.2012.02.014 

Please cite this article in press as: A. Takahashi, et al., Pathological changes in tight junctions and potential applications into therapies, Drug Discov Today (2012), doi:10.1016/j.drudis.2012.02.014

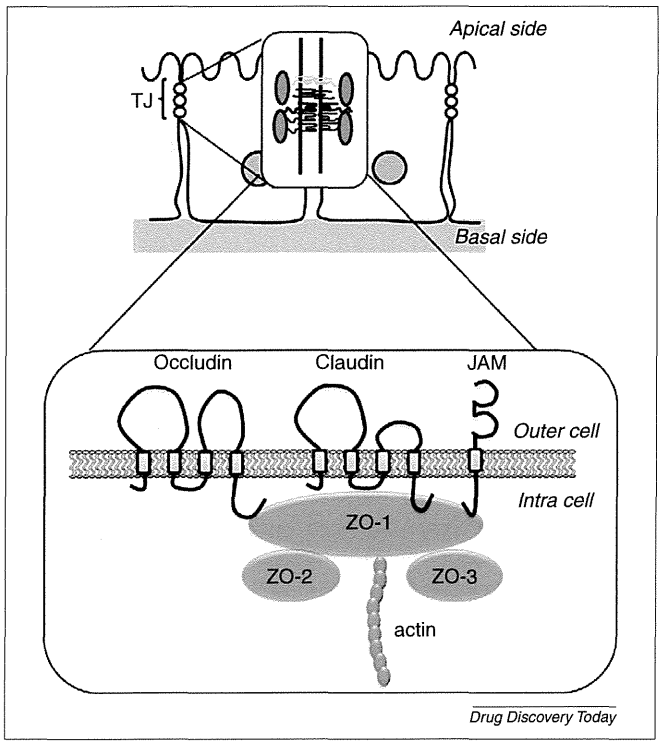


**FIGURE 1**

The epithelial barrier. Occludin, a tetra-transmembrane protein, was the first TJ-constituting protein identified [19]. Claudin was the second [21]. Claudins comprise a tetra-transmembrane protein family of 27 members. JAMs are glycosylated transmembrane proteins that belong to the immunoglobulin superfamily [4]. ZO-1, ZO-2 and ZO-3 are membrane-associated guanylate kinase proteins composed of a PSD95/Dlg/ZO-1 domain, an SH3 domain, a guanylate kinase domain, an acidic domain and an actin-binding region [68]. *Abbreviations*: JAMs: junctional adhesion molecules; TJ: tight junction;

unanchored. Adjacent epithelial cells are joined by occluding junctions called TJs. TJs have pivotal roles in separating the inside of the body from the outside environment, and in separating the inside and outside of tissues. TJs also function as a fence by preventing the free movement of apical membrane components and basal membrane components in epithelial cells.

TJs are intercellular sealing components located at the apical-most part of lateral membranes between adjacent epithelial cells and endothelial cells [17]. Adjacent TJ strands laterally associate with each other to form a paired strand thereby eliminating the intercellular space. Freeze fracture electron microscopy analysis revealed that TJs are continuous anastomosing intramembranous particle strands or fibrils with complementary grooves [3]. TJs are composed of transmembrane proteins, such as claudins, occludin and JAMs, in addition to cytoplasmic plaque proteins, including ZO-1, ZO-2, ZO-3 and cingulin [18].

### *Integral membrane proteins*

Occludin was the first integral membrane protein identified in TJs [19]. Occludin has four transmembrane domains and has a molecular mass of approximately 65 kDa. Deletion of occludin does not affect the structure and function of TJs [20]. Claudins were the second integral membrane proteins identified in TJs [21]. Claudins comprise a multigene family with at least 27 members [7]. Claudins are 21–28-kDa proteins with tetratransmembrane domains. Claudins are key components in the structure and function of TJs [5,6]. A series of cellular analysis and knockout mouse analysis has clarified the roles of claudins in TJs [5,22].

### *Cytoplasmic proteins*

ZO-1 was the first identified TJ-associated protein [23]. ZO-1, ZO-2 and ZO-3 contain PDZ-domains and the membrane-associated guanylate kinase domain. ZO-1, ZO-2 and ZO-3 are involved in formation of the TJ seal; they bind to the C-terminal cytoplasmic domain of occludin and claudins through the ZO PDZ domains [13]. ZO-1 and ZO-2 are crucial components for the definition of TJ formation [11].

### *Tricellular tight junctions*

There are two types of TJs in epithelial cell sheets: bicellular and tricellular [2,24,25]. Occludin, claudins and JAMs are components of bicellular TJs. Tricellulin (approximately 65 kDa) is the only integral membrane component in tricellular TJs [8]. Tricellulin contains four transmembrane domains and shows structural similarity with occludin. Tricellulin is highly concentrated in tricellular TJs, but it is also localized in bicellular TJs [8,26]. Lipolysis-stimulated lipoprotein, a tricellular TJ-associated protein, defines tricellular contacts in epithelial cell sheets [12].

## Mucosal barrier

The intestinal epithelium is where nutrients derived from food are absorbed, and it is also the first line of defense against microorganisms and xenobiotics. Regulation of the epithelial barrier is crucial for mucosal homeostasis. Recently, two intestinal epithelium proteins that regulate the intestinal barrier were identified.

The first protein is guanylyl cyclase C (GCC), which is a transmembrane receptor for the endogenous peptides guanylin and uroguanylin and for bacterial heat-stable enterotoxins [27]. GCC signaling has a pivotal role in the regulation of intestinal fluid and electrolyte homeostasis [28]. GCC-knockout mice show increased intestinal permeability, and GCC-knockdown in Caco-2 cells disrupts TJ integrity. This disruption of the TJ barrier is accompanied by phosphorylation of myosin II regulatory light chains, which induces TJ disassembly. GCC signaling is therefore involved in regulation of the TJ barrier [29].

The second intestinal membrane protein is matriptase. Matriptase is an integral membrane protein with trypsin-like serine protease activity and is a member of the type II transmembrane serine protease family [30]. It is widely expressed in all epithelia, and it is expressed in epithelial cells in the gastrointestinal tract [30]. Loss of matriptase reduces epithelial barrier integrity and enhances paracellular permeability. Matriptase facilitates claudin-2 loss from TJ complexes by indirect regulation of claudin-2 protein turnover by atypical protein kinase C zeta. Interestingly, matriptase does not affect some of the other TJ components, such as claudin-1, claudin-3, claudin-4, claudin-8, ZO-1, or E-cadherin [31].

These findings indicate that GCC signaling and matriptase might be potent targets for the treatment of intestinal disorders whose pathogenesis is disruption of the intestinal barrier function leading to mucosal inflammation and immune activation.



Please cite this article in press as: A. Takahashi, et al., Pathological changes in tight junctions and potential applications into therapies, Drug Discov Today (2012), doi:10.1016/j.drudis.2012.02.014

## TJ dynamics

TJs are complexes of transmembrane and peripheral membrane proteins, including occludin, claudins, ZO-1 and ZO-2 [6]. The TJ structure is highly dynamic and undergoes continuous remodeling through unique kinetics [32]. The properties of TJs are determined by these dynamics [33].

Occludin S408 dephosphorylation reduces paracellular cation influx by stabilizing the occludin–ZO-1 interaction, leading to enhancement of claudin-1 and claudin-2 exchange and reduction of their pore formation at the TJ. By contrast, occludin S408 phosphorylation enhances homotypic occludin–occludin interactions, leading to the release of ZO-1 and formation of claudin-1- and claudin-2-based pores. Therefore, occludin S408 phosphorylation is a key factor in the remodeling of the claudin–occludin–ZO-1 interaction [34].

Claudin-1 is stably localized in TJs [35]. Most occludin is mobile and diffused within the junctional membrane. By contrast, most ZO-1 is continuously exchanged between the membrane and cytosol pools [34]. Fluorescence recovery after photo-bleaching (FRAP) analysis provided new insights into the dynamics of TJs. The perijunctional actomyosin ring contributes to myosin light chain kinase (MLCK)-dependent TJ regulation. FRAP analysis showed that TJ-associated ZO-1 exists in three pools: a fixed pool, a fast exchangeable pool associated with the cytosolic pool, and a slow exchangeable pool associated with the cytosolic pool. The exchange between the TJ pools and the cytosolic pool is regulated by MLCK [36]. Claudin dynamics differ depending on the particular claudin. Claudins forming TJ strands showed slower dynamics than those not forming TJ strands. Distinct claudin stabilities might affect how TJs regulate paracellular permeability by altering paracellular flux and paracellular ion permeability [37].

These insights into the dynamics of TJs address the molecular mechanism of paracellular homeostasis and will hopefully lead to the development of TJ-targeted tissue-specific and solute-specific drug delivery systems.

## Epithelial barrier as the first line of defense against pathological microorganisms

The human mucosa has a surface area equivalent to 1.5 tennis courts. This large surface area means that there is significant risk of infection by pathological microorganisms; therefore, homeostasis of the epithelial barrier is important. Indeed, some pathogens modulate the epithelial barrier to facilitate easy and widespread infection (Fig. 2a).

### *Modulation of the epithelial barrier by pathogens*

Human immunodeficiency virus-1 (HIV-1) infection is often associated with increased permeability of mucosal epithelial cells. Viral envelope glycoprotein (gp)120 is a crucial viral protein that increases the permeability of the epithelial barrier. When HIV-1 binds to cells it induces production of TNF-α, leading to a decrease in mucosal epithelial barrier integrity and spread of HIV-1 infection [38].

Atopic dermatitis (AD) is the most common inflammatory skin disease [39], and susceptibility to cutaneous infections is increased in AD patients. Widespread skin infection by the herpes simplex virus (HSV) causes severe viral complications, such as eczema herpeticum in AD patients. Defects in the epidermal TJ barrier

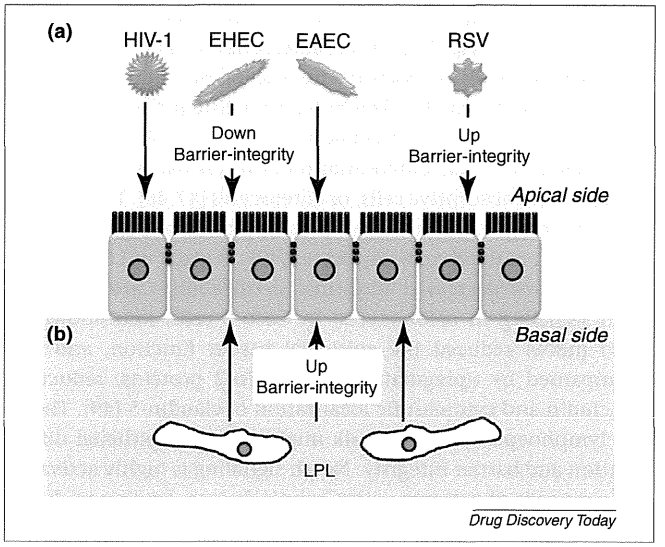


**FIGURE 2**

Regulation of the first line of defense, the epithelial barrier. **(a)** Pathological microorganism–epithelial barrier interaction. Infection of epithelial cells by HIV-1, EHEC, or EAEC decreased epithelial barrier integrity [38,41,42]. By contrast, RSV infection increased the barrier function [44]. **(b)** Lymphocyte–epithelial barrier interaction. LPLs regulate the integrity of the epithelial barrier via direct interaction with epithelial cells through notch signaling [49]. *Abbreviations*: EAEC: enteroaggregative *Escherichia coli*; EHEC: enterohemorrhagic *Escherichia coli*; HIV-1: human immunodeficiency virus-1; LPLs: lamina propria lymphocytes; RSV: respiratory syncytial virus.

increase the susceptibility of patients with AD to widespread subcutaneous infection with HSV or other viral pathogens [40]. In the early stage of infection with enterohemorrhagic *Escherichia coli* (EHEC), non-bloody diarrhea occurs in the absence of shiga toxin. EHEC infection increases expression of claudin-2 and redistribution of claudin-3 and occludin. These changes correlate with increased intestinal permeability [41]. Infection by enteroaggregative *Escherichia coli* (EAEC) causes dissociation of claudin-1 from the TJs between epithelial cells, leading to disruption of the TJ barrier [42]. By contrast, respiratory syncytial virus (RSV) increases TJ integrity. RSV is the major cause of bronchitis, asthma and severe lower respiratory tract diseases in infants and young children [43]. RSV infection induces expression of claudin-4 and occludin in human nasal epithelial cells. Induction of TJ components has a crucial role in epithelial cellular polarity, leading to budding of the virus from the epithelial apical surface [44]. Therefore, prevention of TJ barrier modulation by pathogens might be a viable therapeutic strategy.

### *Lymphoepithelial cross talk in the epithelial barrier*

Mucosa-associated lymphoid tissues (MALTs) are lymphoid immune tissues that are located in the mucosal epithelium. By activating mucosal immune responses, they function as the first line of defense against pathogens invading the body through the epithelium [45]. MALTs comprise gut-associated lymphoid tissues, nasopharynx-associated lymphoid tissues and bronchus-associated lymphoid tissues. MALTs contain lymphocytes, M cells, T cells, B cells and antigen-presenting cells. Recently, lamina propria lymphocytes (LPLs) underlying the intestinal epithelium have





Please cite this article in press as: A. Takahashi, et al., Pathological changes in tight junctions and potential applications into therapies, Drug Discov Today (2012), doi:10.1016/j.drudis.2012.02.014

been shown to have a crucial role in the homeostasis of the epithelial barrier (Fig. 2b). Direct interaction of LPLs with intestinal epithelial cells is essential for the barrier function of the intestinal epithelium [46]. The notch signaling pathway regulates cell fate decisions through cell–cell interactions [47]. Notch signaling determines the differentiation of intestinal stem cells into secretory cells, absorptive cells, or enterocytes [47,48]. The absence of LPLs in mice causes increased intestinal permeability and a lack of activation of notch in colonocytes [49]. Transfer of LPLs to LPL-deficient mice decreased intestinal permeability and activated notch signaling in colonocytes. In Caco-2 cells, knockdown of notch mRNA reduced the epithelial barrier function, and was accompanied by upregulation of claudin-2 proteins, reduction of occludin and cytoplasmic localization of claudin-5 [49]. Therefore, lymphoepithelial cross talk might regulate epithelial differentiation and barrier integrity. Notch signaling is highly activated in the mucosa of patients with Crohn's disease, leading to dysregulation of the differentiation of epithelial cells [49]. Normalization of disruption of this cross talk might be a potent strategy for treating immune-mediated intestinal disorders.

## Proof-of-concept for TJ-targeted drug development

As mentioned in the introduction, epithelial cells are a potent target for drug development. TJ-targeted drug development has been attempted [14,50], and proof-of-concepts for TJ-targeted drug absorption, cancer targeting and mucosal vaccination have been established. Recent findings indicate that TJ-targeted therapy for hepatitis C virus (HCV), diabetes and inflammatory diseases might be possible.

### *HCV infection*

A total of 170 million people worldwide are infected with the HCV. Hepatitis C is the leading cause of chronic liver inflammation, cirrhosis and cancer. Claudin-1 and occludin are co-receptors for HCV infection, indicating that binders to claudin-1 or occludin might be potent inhibitors of HCV entry [16]. DNA immunization enabled successful preparation of monoclonal anti-claudin-1 antibodies against the extracellular loop of claudin-1, and these anti-claudin-1 antibodies prevented HCV infection. Antibodies effectively blocked cell entry of highly infectious escape variants of HCV that were resistant to neutralizing antibodies [51]. When hepatitis C patients reach end-stage liver failure, liver transplantation is the only choice for curative treatment; however, reinfection of the transplanted liver by HCV often occurs. There is a significant correlation between hepatic levels of claudin-1 and occludin and HCV reinfection after liver transplantation [52]. Inhibition of HCV reinfection of the transplanted liver by using anti-claudin-1 antibodies might be a potent treatment for patients with liver transplantation.

### *Diabetic retinopathy*

Breakdown of the blood–retinal barrier (BRB) is a hallmark of diabetic retinopathy [53]. Alterations to the BRB occur early in the progression of diabetic retinopathy and eventually lead to macular edema, which is responsible for vision loss [54]. Diabetic patients show elevated levels of TNF-α in the vitreous humor. TNF-α increases the permeability of retinal endothelial cells. TNF-α decreases ZO-1 and claudin-5 expression and alters cellular localization of ZO-1 and claudin-5 [55]. Thus, regulation of BRB-integrity might be a potent strategy for treating vision loss owing to diabetes. Indeed, a chemical already in clinical use for the treatment of diabetic retinopathy, calcium dobesilate, attenuates the decrease in occludin and claudin-5 and prevents BRB breakdown [56]. Berberine, a plant alkaloid, has also been used for the treatment of diabetes. Berberine prevents barrier defects in retinal epithelial cells [57]. Inducers of occludin and claudin-5 or promoters of TJ integrity could be a potent treatment for diabetic retinopathy.

### *Inflammatory diseases*

Berberine has been also used in the treatment of gastroenteritis and diarrhea. TNF-α disrupts TJ integrity in inflammatory bowel diseases (IBD). Regulation of the TNF-α-dependent signaling pathway is a potent strategy for the treatment of IBD. TNF-α removes claudin-1 from TJs and induces claudin-2 expression, leading to disruption of the TJ barrier. Attenuation of TNF-α signaling is a potent strategy for IBD therapy. Berberine also attenuates TNF-α-induced TJ barrier defects by removing claudin-1 and inducing claudin-2 expression [58]. Spontaneous colitis was observed in interleukin (IL)-10−/− mice in which paracellular permeability was increased in conjunction with decreased expression and redistribution of ZO-1, occludin and claudin-1. Treatment with a probiotic, *Lactobacillus plantarum*, restored expression of TJ components and TJ integrity, resulting in prevention of bacterial translocation and proinflammatory responses in IL-10−/− mice [59]. Recovery of TJ integrity might be a potent strategy for inflammatory intestinal diseases. Ouabain, which is an inhibitor of $Na^+$, $K^+$-ATPase, increased TJ integrity through signaling pathways involving c-Src and ERK1/2 and by modulating the expression of claudin-1, claudin-2 and claudin-4 [60,61]. Several natural products have been found to be therapeutically useful against epithelial barrier defects.

### *Paracellular drug transport*

The claudin protein family comprises 27 members [7]. Claudins form homo- and hetero-type strands in the lateral membrane. Adjacent claudin-based TJ strands associate with each other, leading to sealing of the intercellular space. The combination of the claudin members is a determinant factor for the properties of the TJ barrier [5]. These findings suggest that optimization of claudin modulators with narrow-specificity in certain cases, or broad-specificity in other cases, might regulate solute- and tissue-specificity in paracellular transport. The most important issue in TJ-targeted drug absorption is the development of claudin modulators. Claudin is an integral membrane protein with a tetra-transmembrane domain. Claudin binders are the first choice for claudin modulators. The first extracellular loop contains approximately 50 amino acids and the second contains approximately ten amino acids. Claudins are hydrophobic proteins, and preparation of a recombinant protein is only currently possible for claudin-4 [62]. Therefore, the development of claudin binders, including antibodies, has been slow. Budded baculoviruses display functional forms of membrane proteins on their surface [63]. Claudin-displaying budded baculoviruses possess a native form of claudin and can be used as a screening system for claudin binders [64]. Functional membrane proteins are heterogeneously expressed on


Please cite this article in press as: A. Takahashi, et al., Pathological changes in tight junctions and potential applications into therapies, Drug Discov Today (2012), doi:10.1016/j.drudis.2012.02.014

budded baculoviruses [63]. Functional information using FRAP analysis will enable development of a screening system for claudin modulators with narrow- or broad-specificity using the heterogenous claudin-displaying baculoviral system. We predict that, in the near future, proof-of-concept for tissue- and solute-specific paracellular transport by modulating the claudin-barrier will be demonstrated.

Coupling of transcellular and paracellular transport systems controls permeability to solutes [65]. Claudin-based TJs function as charge-selective paracellular channels [6]. Claudin-15 is responsible for transepithelial permeability to extracellular monovalent cations, especially $Na^+$. Claudin-15-deficient mice exhibit low luminal $Na^+$ levels and low glucose absorption in the intestine, indicating that paracellular transport of $Na^+$ through claudin-15-based TJ strands might be coupled to transcellular transport of glucose through a glucose transporter [66]. These findings suggest that modulation of the claudin-mediated paracellular transport of solutes might regulate the transcellular transport of drugs through a transporter.

## Concluding remarks

To our knowledge, the first report of TJ-targeted drug development was the discovery in 1961 of enhanced mucosal absorption of drugs by co-administration of ethylenediaminetetraacetic acid [67]. TJs were identified in 1963 [17]. Modulation of the TJ-barrier has been a major strategy for enhancing mucosal absorption; however, the biochemical structure of TJs was unclear until 1998. Until that year, absorption enhancers were screened mainly by modulating epithelial cell sheets. Recent imaging studies have begun to reveal the dynamics of TJs and also how these dynamics are regulated [36,37]. Future detailed analyses using FRAP will provide us with new insights into strategies for modulation of the TJ barrier. In addition to TJ-modulated drug absorption, TJ-targeted therapy for HCV infection and diabetic retinopathy has recently been proved effective [51,56]. The questions of how TJ dynamics are regulated, and how expression of TJ components is regulated are still to be answered. The molecular pathology of deregulation of the TJ barrier is not yet fully understood. TJ-targeted drug development has been spearheaded by rapid progress in our understanding of the biology of the TJ barrier.

## Acknowledgements

This work was supported in part by a Grant-in-Aid for Scientific Research from the Ministry of Education, Culture, Sports, Science and Technology, Japan (21689006) and by Health and Labor Sciences Research Grants from the Ministry of Health, Labor and Welfare of Japan. AT and HS are supported by Research Fellowships of the Japan Society for the Promotion of Science for Young Scientists.

## References

1 Anderson, J.M. and Van Itallie, C.M. (1995) Tight junctions and the molecular basis for regulation of paracellular permeability. *Am. J. Physiol.* 269 (4 Pt 1), G467–G475
2 Gumbiner, B. (1993) Breaking through the tight junction barrier. *J. Cell Biol.* 123, 1631–1633
3 Staehelin, L.A. (1973) Further observations on the fine structure of freeze-cleaved tight junctions. *J. Cell Sci.* 13, 763–786
4 Chiba, H. *et al.* (2008) Transmembrane proteins of tight junctions. *Biochim. Biophys. Acta* 1778, 588–600
5 Furuse, M. and Tsukita, S. (2006) Claudins in occluding junctions of humans and flies. *Trends Cell Biol.* 16, 181–188
6 Van Itallie, C.M. and Anderson, J.M. (2009) Physiology and function of the tight junction. *Cold Spring Harb. Perspect. Biol.* 1, a002584
7 Mineta, K. *et al.* (2011) Predicted expansion of the claudin multigene family. *FEBS Lett.* 585, 606–612
8 Ikenouchi, J. *et al.* (2005) Tricellulin constitutes a novel barrier at tricellular contacts of epithelial cells. *J. Cell Biol.* 171, 939–945
9 Sanchez-Pulido, L. *et al.* (2002) MARVEL: a conserved domain involved in membrane apposition events. *Trends Biochem. Sci.* 27, 599–601
10 Raleigh, D.R. *et al.* (2010) Tight junction-associated MARVEL proteins marvelD3, tricellulin, and occludin have distinct but overlapping functions. *Mol. Biol. Cell* 21, 1200–1213
11 Umeda, K. *et al.* (2006) ZO-1 and ZO-2 independently determine where claudins are polymerized in tight-junction strand formation. *Cell* 126, 741–754
12 Masuda, S. *et al.* (2011) LSR defines cell corners for tricellular tight junction formation in epithelial cells. *J. Cell Sci.* 124 (Pt 4), 548–555
13 Furuse, M. (2010) Molecular basis of the core structure of tight junctions. *Cold Spring Harb. Perspect. Biol.* 2, a002907
14 Takahashi, A. *et al.* (2011) Claudin as a target for drug development. *Curr. Med. Chem.* 18, 1861–1865
15 Turksen, K. and Troy, T.C. (2011) Junctions gone bad: claudins and loss of the barrier in cancer. *Biochim. Biophys. Acta* 1816, 73–79
16 Zeisel, M.B. *et al.* (2011) Hepatitis C virus entry into hepatocytes: molecular mechanisms and targets for antiviral therapies. *J. Hepatol.* 54, 566–576
17 Farquhar, M.G. and Palade, G.E. (1963) Junctional complexes in various epithelia. *J. Cell Biol.* 17, 375–412
18 Nusrat, A. *et al.* (2000) Molecular physiology and pathophysiology of tight junctions. IV. Regulation of tight junctions by extracellular stimuli: nutrients, cytokines, and immune cells. *Am. J. Physiol.* 279, G851–G857
19 Furuse, M. *et al.* (1993) Occludin: a novel integral membrane protein localizing at tight junctions. *J. Cell Biol.* 123 (6 Pt 2), 1777–1788
20 Saitou, M. *et al.* (1998) Occludin-deficient embryonic stem cells can differentiate into polarized epithelial cells bearing tight junctions. *J. Cell Biol.* 141, 397–408
21 Furuse, M. *et al.* (1998) A single gene product, claudin-1 or -2, reconstitutes tight junction strands and recruits occludin in fibroblasts. *J. Cell Biol.* 143, 391–401
22 Furuse, M. (2009) Knockout animals and natural mutations as experimental and diagnostic tool for studying tight junction functions *in vivo*. *Biochim. Biphys. Acta* 1788, 813–819
23 Stevenson, B.R. *et al.* (1986) Identification of ZO-1: a high molecular weight polypeptide associated with the tight junction (zonula occludens) in a variety of epithelia. *J. Cell Biol.* 103, 755–766
24 Staehelin, L.A. *et al.* (1969) Freeze-etch appearance of the tight junctions in the epithelium of small and large intestine of mice. *Protoplasma* 67, 165–184
25 Friend, D.S. *et al.* (1972) Variations in tight and gap junctions in mammalian tissues. *J. Cell Biol.* 53, 375–412
26 Ikenouchi, J. *et al.* (2008) Loss of occludin affects tricellular localization of tricellulin. *Mol. Biol. Cell* 19, 4687–4693
27 Lin, J.E. *et al.* (2009) Guanylyl cyclase C in colorectal cancer: susceptibility gene and potential therapeutic target. *Future Oncol.* 5, 509–522
28 Lorenz, J.N. *et al.* (2003) Uroguanylin knockout mice have increased blood pressure and impaired natriuretic response to enteral NaCl load. *J. Clin. Invest.* 112, 1244–1254
29 Han, X. *et al.* (2011) Loss of guanylyl cyclase C (GCC) signaling leads to dysfunctional intestinal barrier. *PLoS ONE* 6, E16139
30 Bugge, T.H. *et al.* (2007) Matriptase-dependent cell surface proteolysis in epithelial development and pathogenesis. *Front. Biosci.* 12, 5060–5070
31 Buzza, M.S. *et al.* (2010) Membrane-anchored serine protease matriptase regulates epithelial barrier formation and permeability in the intestine. *Proc. Natl. Acad. Sci. U. S. A.* 107, 4200–4205
32 Ikenouchi, J. *et al.* (2003) Regulation of tight junctions during the epithelium–mesenchyme transition: direct repression of the gene expression of claudins/occludin by Snail. *J. Cell Sci.* 116 (Pt 10), 1959–1967
33 Steed, E. *et al.* (2010) Dynamics and functions of tight junctions. *Trends Cell Biol.* 20, 142–149
34 Raleigh, D.R. *et al.* (2011) Occludin S408 phosphorylation regulates tight junction protein interactions and barrier function. *J. Cell Biol.* 193, 565–582



Please cite this article in press as: A. Takahashi, et al., Pathological changes in tight junctions and potential applications into therapies, Drug Discov Today (2012), doi:10.1016/j.drudis.2012.02.014

35 Sasaki, H. *et al.* (2003) Dynamic behavior of paired claudin strands within apposing plasma membranes. *Proc. Natl. Acad. Sci. U. S. A.* 100, 3971–3976
36 Yu, D. *et al.* (2010) MLCK-dependent exchange and actin binding region-dependent anchoring of ZO-1 regulate tight junction barrier function. *Proc. Natl. Acad. Sci. U. S. A.* 107, 8237–8241
37 Yamazaki, Y. *et al.* (2011) Role of claudin species-specific dynamics in reconstitution and remodeling of the zonula occludens. *Mol. Biol. Cell* 22, 1495–1504
38 Nazli, A. *et al.* (2010) Exposure to HIV-1 directly impairs mucosal epithelial barrier integrity allowing microbial translocation. *PLoS Pathog.* 6, E1000852
39 Beck, L.A. *et al.* (2009) Phenotype of atopic dermatitis subjects with a history of eczema herpeticum. *J. Allergy Clin. Immunol.* 124, 260–269 269 E261–E267
40 De Benedetto, A. *et al.* (2011) Reductions in claudin-1 may enhance susceptibility to herpes simplex virus 1 infections in atopic dermatitis. *J. Allergy Clin. Immunol.* 128, 242–246 E245
41 Roxas, J.L. *et al.* (2010) Enterohemorrhagic *E. coli* alters murine intestinal epithelial tight junction protein expression and barrier function in a Shiga toxin independent manner. *Lab. Invest.* 90, 1152–1168
42 Strauman, M.C. *et al.* (2010) Enteroaggregative *Escherichia coli* disrupts epithelial cell tight junctions. *Infect. Immun.* 78, 4958–4964
43 Bitko, V. and Barik, S. (1998) Persistent activation of RelA by respiratory syncytial virus involves protein kinase C, underphosphorylated IkappaBbeta, and sequestration of protein phosphatase 2A by the viral phosphoprotein. *J. Virol.* 72, 5610–5618
44 Masaki, T. *et al.* (2011) A nuclear factor-kappaB signaling pathway via protein kinase C delta regulates replication of respiratory syncytial virus in polarized normal human nasal epithelial cells. *Mol. Biol. Cell* 22, 2144–2156
45 Kunisawa, J. *et al.* (2008) Immunological commonalities and distinctions between airway and digestive immunity. *Trends Immunol.* 29, 505–513
46 Dahan, S. *et al.* (2009) Lymphoepithelial interactions: a new paradigm. *Ann. N. Y. Acad. Sci.* 1165, 323–326
47 Kopan, R. and Ilagan, M.X. (2009) The canonical Notch signaling pathway: unfolding the activation mechanism. *Cell* 137, 216–233
48 Hermiston, M.L. *et al.* (1993) Chimeric-transgenic mice represent a powerful tool for studying how the proliferation and differentiation programs of intestinal epithelial cell lineages are regulated. *Proc. Natl. Acad. Sci. U. S. A.* 90, 8866–8870
49 Dahan, S. *et al.* (2011) Notch-1 signaling regulates intestinal epithelial barrier function, through interaction with $CD4^+$ T cells, in mice and humans. *Gastroenterology* 140, 550–559
50 Kondoh, M. *et al.* (2008) Targeting tight junction proteins – significance for drug development. *Drug Discov. Today* 13, 180–186
51 Fofana, I. *et al.* (2010) Monoclonal anti-claudin 1 antibodies prevent hepatitis C virus infection of primary human hepatocytes. *Gastroenterology* 139, 953–964 964 E951–E954
52 Mensa, L. *et al.* (2011) Hepatitis C virus receptors claudin-1 and occludin after liver transplantation and influence on early viral kinetics. *Hepatology* 53, 1436–1445
53 Cunha-Vaz, J. *et al.* (1975) Early breakdown of the blood–retinal barrier in diabetes. *Br. J. Ophthalmol.* 59, 649–656
54 The Diabetes Control and Complications Trial Research Group, (1993) The effect of intensive treatment of diabetes on the development and progression of long-term complications in insulin-dependent diabetes mellitus. *N. Engl. J. Med.* 329, 977–986
55 Aveleira, C.A. *et al.* (2010) TNF-alpha signals through PKCzeta/NF-kappaB to alter the tight junction complex and increase retinal endothelial cell permeability. *Diabetes* 59, 2872–2882
56 Leal, E.C. *et al.* (2010) Calcium dobesilate inhibits the alterations in tight junction proteins and leukocyte adhesion to retinal endothelial cells induced by diabetes. *Diabetes* 59, 2637–2645
57 Cui, H.S. *et al.* (2007) Effect of berberine on barrier function in a human retinal pigment epithelial cell line. *Jpn. J. Ophthalmol.* 51, 64–67
58 Amasheh, M. *et al.* (2010) TNFalpha-induced and berberine-antagonized tight junction barrier impairment via tyrosine kinase, Akt and NFkappaB signaling. *J. Cell Sci.* 123 (Pt 23), 4145–4155
59 Chen, H.Q. *et al.* (2010) Lactobacillus plantarum ameliorates colonic epithelial barrier dysfunction by modulating the apical junctional complex and PepT1 in IL-10 knockout mice. *Am. J. Physiol.* 299, G1287–G1297
60 Larre, I. *et al.* (2010) Ouabain modulates epithelial cell tight junction. *Proc. Natl. Acad. Sci. U. S. A.* 107, 11387–11392
61 Larre, I. *et al.* Ouabain modulates ciliogenesis in epithelial cells. *Proc. Natl. Acad. Sci. U. S. A.*, doi:10.1073/pnas.1102617108 (in press)
62 Mitic, L.L. *et al.* (2003) Expression, solubilization, and biochemical characterization of the tight junction transmembrane protein claudin-4. *Protein Sci.* 12, 218–227
63 Sakihama, T. *et al.* (2008) Functional reconstitution of G-protein-coupled receptor-mediated adenylyl cyclase activation by a baculoviral co-display system. *J. Biotechnol.* 135, 28–33
64 Kakutani, H. *et al.* (2011) A novel screening system for claudin binder using baculoviral display. *PLoS ONE* 6, E16611
65 Kapus, A. and Szaszi, K. (2006) Coupling between apical and paracellular transport processes. *Biochem. Cell Biol.* 84, 870–880
66 Tamura, A. *et al.* (2011) Loss of claudin-15, but not claudin-2, causes Na(+) deficiency and glucose malabsorption in mouse small intestine. *Gastroenterology* 140, 913–923
67 Windsor, E. and Cronheim, G.E. (1961) Gastro-intestinal absorption of heparin and synthetic heparinoids. *Nature* 190, 263–264
68 Gonzalez-Mariscal, L. *et al.* (2000) MAGUK proteins: structure and role in the tight junction. *Semin. Cell Dev. Biol.* 11, 315–324


Please cite this article in press as: A. Takahashi, et al., Pathological changes in tight junctions and potential applications into therapies, Drug Discov Today (2012), doi:10.1016/j.drudis.2012.02.014

Biochemical and Biophysical Research Communications 426 (2012) 454–460

Contents lists available at SciVerse ScienceDirect

Biochemical and Biophysical Research Communications

journal homepage: www.elsevier.com/locate/ybbrc

# A simple reporter assay for screening claudin-4 modulators

Akihiro Watari, Kiyohito Yagi, Masuo Kondoh *

*Laboratory of Bio-Functional Molecular Chemistry, Graduate School of Pharmaceutical Sciences, Osaka University, Suita, Osaka 565-0871, Japan*

ARTICLE INFO

*Article history:*
Received 15 August 2012
Available online 27 August 2012

*Keywords:*
Claudin
Tight junction
Reporter assay
Screening
Chemical modulator

ABSTRACT

Claudin-4, a member of a tetra-transmembrane protein family that comprises 27 members, is a key functional and structural component of the tight junction-seal in mucosal epithelium. Modulation of the claudin-4-barrier for drug absorption is now of research interest. Disruption of the claudin-4-seal occurs during inflammation. Therefore, claudin-4 modulators (repressors and inducers) are promising candidates for drug development. However, claudin-4 modulators have never been fully developed. Here, we attempted to design a screening system for claudin-4 modulators by using a reporter assay. We prepared a plasmid vector coding a claudin-4 promoter-driven luciferase gene and established stable reporter gene-expressing cells. We identified thiabendazole, carotene and curcumin as claudin-4 inducers, and potassium carbonate as a claudin-4 repressor by using the reporter cells. They also increased or decreased, respectively, the integrity of the tight junction-seal in Caco-2 cells. This simple reporter system will be a powerful tool for the development of claudin-4 modulators.

© 2012 Elsevier Inc. All rights reserved.

## 1. Introduction

Tight junctions (TJs), the most apical components of intercellular junctional complexes, function as fences that maintain cellular polarity and provide a barrier to regulate intercellular permeability of epithelia [1,2]. Disruption of cellular polarity and the TJ-seal is frequently observed during carcinogenesis and inflammation [3]. Modulation of TJ-seals for drug absorption is now of research interest [4,5]. A series of studies has revealed that TJs are composed of transmembrane proteins (such as occludin and claudins), junction adhesion proteins, and cytoplasmic scaffolding proteins, including ZO-1, ZO-2, and ZO-3 (see reviews [6–8]). Of these, claudins are thought to be the main structural and functional components of TJs.

Claudins, tetra-transmembrane proteins with a molecular mass of approximately 23 kDa, comprise a multigene family containing over 20 members [8]. The barrier-function and the expression patterns of claudin members differ among tissues [6,8,9]. Claudin-1-, -5-, and -11-deficient mice show dysfunction of the epidermal barrier, blood–brain barrier, and blood–testis barrier, respectively [10–12]. The expression levels and the barrier-functions of claudins are often altered in various cancer cells; they can be down-regulated or up-regulated, depending on the type of cancer [13]. Changes in claudin expression have also been observed in the mucosal epithelium under inflammatory conditions [14]. Claudins are thus potent targets for drug development, such as drug delivery, anti-cancer agents, and anti-inflammatory agents.

Since claudins play a role in TJ-seals, modulation of the claudin-barrier is a potent strategy for drug absorption. The carboxyl-terminus of *Clostridium perfringens* enterotoxin (C-CPE) is a modulator of the claudin-barrier [15]. Treatment of cells with C-CPE causes a decrease in claudin-4 proteins in TJs, followed by an enhancement of the paracellular transport of solutes without causing cytotoxicity [15]. C-CPE also enhances jejunal, nasal, and pulmonary absorption of drugs [16]. Thus, proof-of-concept for claudin-targeted drug absorption has been demonstrated. A decrease in claudin-4 in the intestinal epithelium often occurs in colitis [17]. Down-regulation of claudin-4 is also observed in some cancer cells [18]. Induction of claudin-4 is involved in the chemo-preventive effect of nonsteroidal anti-inflammatory drugs [19]. A modulator of claudin-4 expression would therefore be a potent molecule for claudin-targeted drug absorption and drug development for some inflammatory diseases and cancers. However, an effective system to screen for claudin modulators is lacking.

Here, we developed a simple system to monitor claudin-4 expression using a reporter gene, and we screened chemical claudin-4 modulators.

*Abbreviations:* TJs, tight junctions; C-CPE, the carboxyl terminus of *Clostridium perfringens* enterotoxin; TGF-β, transforming growth factor-β; EGF, epidermal growth factor; PMA, phorbol 12-myristate 13-acetate; DMSO, dimethyl sulfoxide; PCR, polymerase chain reaction; RT-PCR, reverse transcription-PCR; GAPDH, glyceraldehyde 3-phosphate dehydrogenase; qPCR, quantitative PCR; SDS, sodium dodecyl sulfate; SDS-PAGE, SDS-polyacrylamide gel electrophoresis; TER, transepithelial electric resistance.

* Corresponding author. Fax: +81 6 6879 8199.
*E-mail address:* masuo@phs.osaka-u.ac.jp (M. Kondoh).

0006-291X/$ - see front matter © 2012 Elsevier Inc. All rights reserved.
http://dx.doi.org/10.1016/j.bbrc.2012.08.083

## 2. Materials and methods

### 2.1. Reagents and cells

Recombinant human transforming growth factor-β (TGF-β) and epidermal growth factor (EGF) were purchased from R&D systems (Minneapolis, MN) and Peprotech Inc. (Rocky Hill, NJ), respectively. The recombinant proteins were dissolved in water and stored at −80 °C before use. Phorbol 12-myristate 13-acetate (PMA) were dissolved in dimethyl sulfoxide (DMSO) and stored at −20 °C before use. List of the chemicals used in this study for screening for claudin-4 modulator is shown in Table 1. All reagents were of research grade.

MCF-7, and Caco-2 cells were cultured in Dulbecco's modified minimal essential medium supplemented with 10% fetal bovine serum in 5% $CO_2$ at 37 °C. MCF-7 cells were obtained from the RIKEN cell bank (Ibaragi, Japan). Caco-2 cells were obtained from the American Type Culture Collection (Manassas, VA). MCF-7 cells stably expressing snail or HRasV12 were prepared by infection with a recombinant retroviral vector coding for snail or HRasV12 gene.

### 2.2. Preparation of a reporter plasmid

Genomic DNA was extracted from MCF-7 cells by using a genomic DNA isolation kit (Sigma–Aldrich, St. Louis, MO). The claudin-4 promoter region was cloned by polymerase chain reaction (PCR) using genomic DNA as a template and paired primers (forward primer, 5′-GCGCTAGCGGTTGCCCCCTGGCCTTAAC-3′; reverse primer, 5′-CGCTCGAGGTCCACGGGAGTTGAGGACC-3′). The resultant fragments (500 bp) were subcloned into the pGV-B2 vector encoding the luciferase gene (Toyobo, Osaka, Japan). The sequence of the claudin-4 promoter region was confirmed.

### 2.3. A transient expression of transfection snail or HRasV12 gene

Transfection was performed with FuGENE HD (Roche, Mannheim, Germany) according to the manufacturer's protocol. Briefly, cells were seeded onto 24-well plates. When the cells reached to 80% confluent cell density, 20 μl of medium containing 0.6 μl of FuGENE HD and 200 ng of plasmid carrying snail or HRasV12 gene was added to the wells. After 48 h of transfection, the luciferase activity of the cell lysates was measured as described below.

### 2.4. Luciferase assay

Luciferase activity was measured using a commercial available luciferase assay system (Toyo Ink, Tokyo, Japan). Cells were lysed with a cell lysis reagent, LCβ (Toyo Ink). The cell lysates were then centrifuged at *18,000g* for 5 min. The luciferase activity in the resulting supernatant was measured using a TriStar LB 941 microplate reader (Berthold, Wildbad, Germany).

### 2.5. Establishment of a stable reporter cell line

MCF-7 cells were transfected with the reporter plasmid and a plasmid carrying the puromycin resistance gene. Stable transfectants were selected in the presence of puromycin.

### 2.6. Screening for claudin-4 modulators

The clone 35 cells were seeded onto 96-well plates at a density of $4 \times 10^4$ cells/well. On the following day, vehicle or compound was added, and the cells were cultured for an additional 24 h. The luciferase activity in the cells was then measured as described above.

### 2.7. Cytotoxicity assay

Clone 35 cells or Caco-2 cells were seeded onto a 96-well plate at a density of $4 \times 10^4$ or $6 \times 10^4$ cells/well, respectively. On the following day, cells were treated with chemicals at the indicated periods. The cell viability was measured by using a WST-8 assay kit (Nacalai, Kyoto, Japan).

### 2.8. Reverse transcription–PCR (RT–PCR) analysis

RT reaction and PCR amplification were performed with a cDNA synthesis kit (Roche, Mannheim, Germany) and ExTaqTM (Takara, Shiga, Japan), respectively, according to the manufacturer's instructions. Briefly, total RNA was prepared with TRIzol reagent (Invitrogen, Carlsbad, CA). For reverse transcription, 5 μg of total RNA was used. PCR was performed for 23 cycles for claudin-4 (94 °C for 30 s, 55 °C for 15 s, 72 °C for 30 s) and for 20 cycles for GADPH (94 °C for 30 s, 55 °C for 15 s, 72 °C for 60 s). The PCR products were separated by use of agarose gel electrophoresis and stained with ethidium bromide. The sequences of the primers are as follows: forward primer for claudin-4, 5′-CAACATTGTCACCTCGCAGACCATC-3′; reverse primer for claudin-4, 5′-TATCACCATAAGGCCGGCCAACAG-3′; forward primer for glyceraldehyde 3-phosphate dehydrogenase (GAPDH), 5′-TCTTCACCACCATGGAGAAG-3′; reverse primer for GAPDH, 5′-ACCACCTGGTGCTCAGTGTA-3′.

### 2.9. Quantitative PCR (qPCR) analysis

qPCR was performed with SYBR Premix Ex Taq II (Takara) using an Applied Biosystems StepOne Plus (Applied Biosystems, Foster City, CA). Relative quantification was performed against a standard curve and the values were normalized against the input determined for the housekeeping gene, GAPDH. The primer sequences used for qPCR were as follows: forward primer for claudin-4, 5′-TTGTCACCTCGCAGACCATC-3′ and reverse primer for claudin-4, 5′-CAGCGAGTCGTACACCTTG-3′; forward primer for GAPDH, 5′-GGTGGTCTCCTCTGACTTCAACA-3′ and reverse primer for GAPDH, 5′-GTGGTCGTTGAGGGCAATG-3′.

### 2.10. Western blot analysis

Cells were lysed with RIPA buffer (0.15 M NaCl, 50 mM Tris–HCl, pH 7.4, 1 mM ethylenediaminetetraacetic acid, 1% Triton X-100, 1% sodium deoxycholate, 0.1% sodium dodecyl sulfate (SDS), 1% protease inhibitor cocktail [Sigma–Aldrich]). The cell lysates were subjected to 15% SDS–polyacrylamide gel electrophoresis (SDS–PAGE), followed by blotting onto polyvinylidene difluoride membrane. The membranes were incubated with anti-claudin-4 mouse monoclonal (Zymed, South San Francisco, CA) and anti-β-actin mouse monoclonal (Sigma–Aldrich) antibodies, respectively, and subsequently treated with horseradish peroxidase-conjugated anti-mouse IgG (Zymed). The reactive bands were detected by using an enhanced chemiluminescence reagent (GE Healthcare, Buckinghamshire, UK).

### 2.11. Transepithelial electric resistance (TER) assay

Caco-2 cells were seeded into Transwell™ chambers (Corning, NY) at a density of $8 \times 10^4$ cells/well. On 7 days after the seeding or when TER values reached a plateau, claudin-4 inducers (thiabendazole, carotene, or curcumin) or claudin-4 repressor (potassium carbonate), respectively, was added. The TER values were then monitored at 0, 24, and 48 h using a Millicell-ERS epithelial

**Table 1**
Chemicals used in this study as screening sources.

| Sample number | Sample name | Concentration[a] | Relative luciferase activity[b] |
|---|---|---|---|
| 1 | Tartrazine | 10 mM | 1.29 |
| 2 | Potassium nitrate | 1 mM | 0.94 |
| 3 | Potassium carbonate | 10 mM | 0.56 |
| 4 | Sodium chlorous | 10 mM | 0.95 |
| 5 | Zinc sulfate | 0.1 mM | 0.95 |
| 6 | New coccine | 0.01 mM | 0.98 |
| 7 | Amaranth (Bordeaux S) | 1 mM | 1.34 |
| 8 | Allura red AC | 1 mM | 1.49 |
| 9 | Sunset yellow FCF | 1 mM | 1.59 |
| 10 | Potassium hydroxide | 1 mM | 0.83 |
| 11 | L-ascorbic acid | 1 mM | 1.02 |
| 12 | Sodium nitrite | 10 mM | 0.91 |
| 13 | Propionic acid | 0.0001% | 0.82 |
| 14 | Sodium carbonate | 1 mM | 0.91 |
| 15 | Zinc gluconate | 0.01% | 1.76 |
| 16 | Benzoic acid | 0.01 mM | 1.3 |
| 17 | Sorbic acid | 1 mM | 1.51 |
| 18 | Aspartame | 1 mM | 1.59 |
| 19 | Dibutylhydroxytoluene | 0.01 mM | 1.81 |
| 20 | Allyl isothiocyanate | 0.0001% | 1.72 |
| 21 | Saccharin | 1 mM | 1.5 |
| 22 | L-Ascorbyl palmitate | 1 mM | 1.21 |
| 23 | Hydroxy biphenyl | 0.01 mM | 1.87 |
| 24 | Aluminium potassium sulfate | 0.1 mM | 0.94 |
| 25 | L-Lysine | 10 mM | 1.42 |
| 26 | Calcium pantothenate | 10 mM | 1.61 |
| 27 | Carrageenin | 0.01 mM | 1.56 |
| 28 | Tartaric acid | 1 mM | 1.01 |
| 29 | Sodium acetate | 10 mM | 1.02 |
| 30 | Glycine | 10 mM | 1.68 |
| 31 | Sodium alginate | 10 mM | 1.52 |
| 32 | Ammonium chloride | 10 mM | 1.91 |
| 33 | Magnesium sulfate | 10 mM | 1.56 |
| 34 | 5-Ribonucleotide | 0.001 mM | 1.15 |
| 35 | Calcium chloride | 1 mM | 1.62 |
| 36 | Valine | 10 mM | 1.08 |
| 37 | Erythrosine | 0.01 mM | 1.22 |
| 38 | Annatto | 0.01 mM | 1.96 |
| 39 | Maltitol | 10 mM | 1.44 |
| 40 | Sodium dehydroacetate | 1 mM | 1.98 |
| 41 | Nicotinic acid | 1 mM | 1.55 |
| 42 | Isoleucine | 1 mM | 1.06 |
| 43 | Mannitol | 10 mM | 1.29 |
| 44 | Ascorbic acid (Vitamin C) | 10 mM | 1.17 |
| 45 | Phenylalanine | 1 mM | 0.95 |
| 46 | Gallic acid | 0.1 mM | 1.41 |
| 47 | Erythorbic acid (Sodium isoascorbate) | 1 mM | 1.03 |
| 48 | Magnesium chloride | 0.1% | 1.26 |
| 49 | Cochineal extract | 0.1% | 1.02 |
| 50 | Calcium dihydrogen pyrophosphate | 1 mM | 1.1 |
| 51 | Calcium citrate | 0.01 mM | 0.92 |
| 52 | Polyvinyl acetate | 0.1 mM | 1.13 |
| 53 | Fumaric acid | 0.01 mM | 1.24 |
| 54 | Sodium methyl *p*-hydroxybenzoate | 1 mM | 2.04 |
| 55 | Tocophenol (Vitamin E) | 0.0001% | 2.14 |
| 56 | Rennet | 0.01% | 0.89 |
| 57 | Ionone | 0.01% | 1.15 |
| 58 | Isoeugenol | 0.001% | 1.15 |
| 59 | Allyl isosulfocyanate | 0.001% | 1.06 |
| 60 | Propylene glycol | 0.1% | 0.87 |
| 61 | Ethyl isovalerate | 0.001% | 0.89 |
| 62 | Pectin | 0.001% | 0.98 |
| 63 | Cysteine | 0.01 mM | 0.76 |
| 64 | Tragacanth gum | 0.01% | 0.83 |
| 65 | Thiamin | 0.1% | 1.15 |
| 66 | Gum arabic | 0.01% | 0.91 |
| 67 | Cellulose | 0.001% | 0.84 |
| 68 | Thiabendazole | 0.1 mM | 3.24 |
| 69 | Isopropyl citrate | 10 mM | 1.04 |
| 70 | γ-oryzanol | 0.01% | 1.02 |
| 71 | Calcium carbonate | 0.001% | 0.857 |
| 72 | Propylene glycol alginate | 0.01% | 0.87 |
| 73 | Chlorophyll | 0.1% | 1.02 |
| 74 | Sodium chondroitin sulfate | 0.1% | 1.04 |

**Table 1** (*continued*)

| Sample number | Sample name | Concentration[a] | Relative luciferase activity[b] |
|---|---|---|---|
| 75 | Biphenyl | 0.1 mM | 0.99 |
| 76 | Sodium cytidylic acid | 1 mM | 0.77 |
| 77 | Stevia rebaudiana | 0.01% | 0.96 |
| 78 | Calcium stearoyl lactylate | 0.01% | 0.83 |
| 79 | Ferrous sulfate | 0.1 mM | 1.37 |
| 80 | Calcium sulfate | 0.1 mM | 0.93 |
| 81 | Benzoyl peroxide | 0.1 mM | 1.13 |
| 82 | Dibenzoyl thiamine | 1 mM | 0.88 |
| 83 | Carotene | 0.1 mM | 2.09 |
| 84 | Guar gum | 0.001% | 0.84 |
| 85 | Xanthan gum | 0.001% | 0.77 |
| 86 | Curcumin | 0.01 mM | 2.0 |

[a] The chemical concentrations were set at the maximum level to show no cytotoxicity.
[b] The relative luciferase activities were calculated as the ratio of that in the chemical-treated cells to that in the vehicle-treated cells. The treatment period was 24 h.

volt-ohmmeter (Millipore Corporation, Billerica, MA). The TER values were normalized to the area of the Caco-2 cell monolayers, and the TER value of a blank chamber was subtracted.

## 3. Results

### *3.1. Preparation of a reporter plasmid encoding a claudin-4-promoter-driven luciferase gene*

As a first step toward developing a simple screening system for claudin-4 modulators, we cloned the promoter region of claudin-4. We searched for a region that was highly conserved among animals by using a UCSC Genome Bioinformatics program and cloned a 500 bp fragment corresponding to −293 to +194 bp of the claudin-4 gene. This 500 bp fragment contained various transcription factor-binding sites: an E-box (−276 to −271, −262 to −257, −221 to −216, −19 to −14, +10 to +14), a smad-binding element (SBE; −212 to −209, −103 to −100, −38 to −35), and Sp1 (−66 to −57, −53 to −44) [20,21], indicating that this region is a potent candidate for a regulatory region of claudin-4 expression. We constructed a reporter expression vector, in which the 500 bp fragment was inserted upstream of a luciferase gene Suppl. Fig. 1A). To

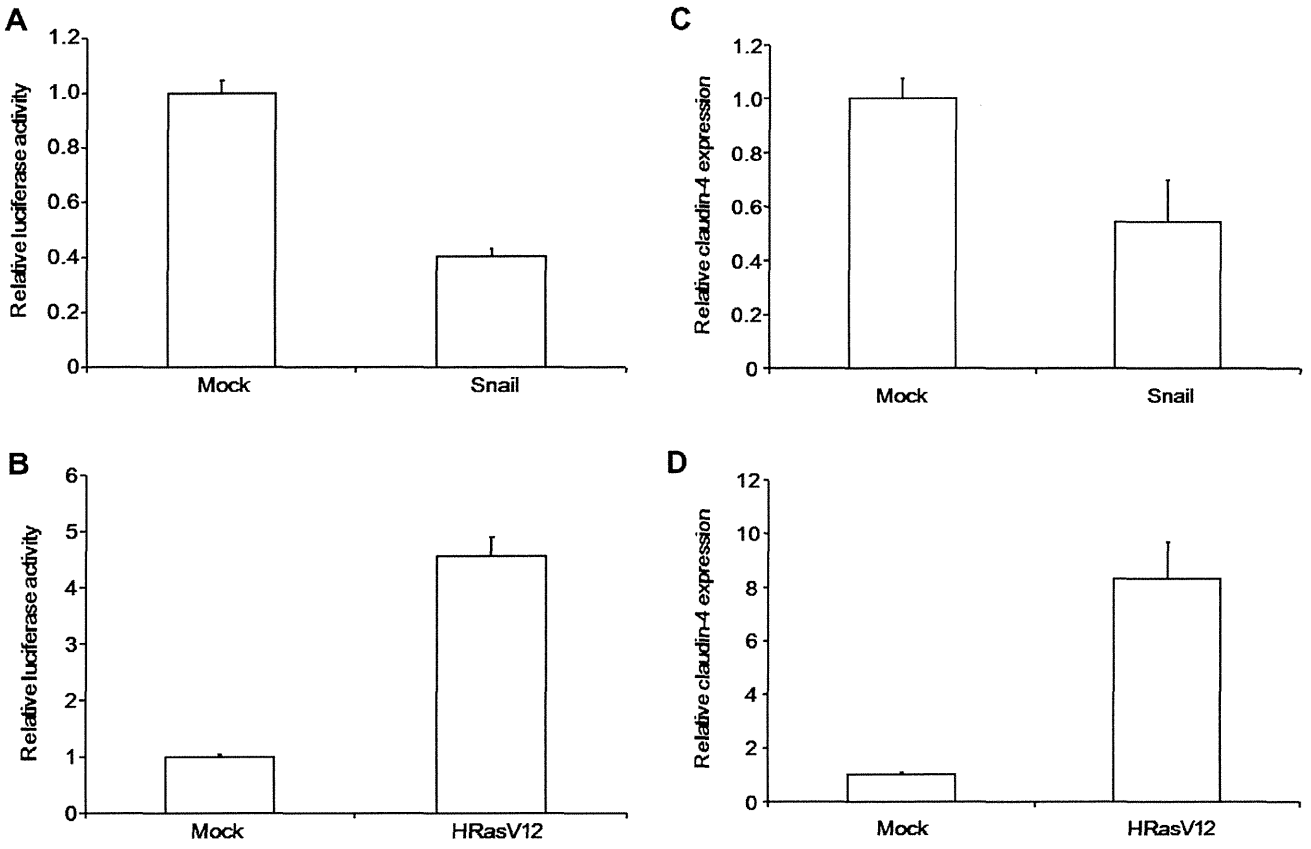


**Fig. 1.** Preparation of a reporter system monitoring claudin-4 expression. (A, B) Effects of snail and HRasV12 on the luciferase activity in transiently expressing cells. Snail-expressing MCF-7 cells (A) or HRasV12-expressing MCF7 cells (B) were transfected with the claudin-4 reporter plasmid. Two days later, the cells were recovered, and the luciferase activity in the lysates was measured. The data are means ± S.D. ($n = 3$). The results are representative of two independent experiments. (C, D) qPCR analysis of claudin-4 expression in transiently expressing cells. After 2 days of the transfection with the claudin-4 reporter plasmid, total RNA was extracted from snail-expressing MCF-7 cells (C) or HRasV12-expressing MCF-7 cells (D). Expression level of claudin-4 of the transfected cells was quantified by qPCR as described in the Section 2. Claudin-4 expression level was shown as ratio to that of the mock cells. The data are means ± S.D. ($n = 3$). The results are representative of two independent experiments.

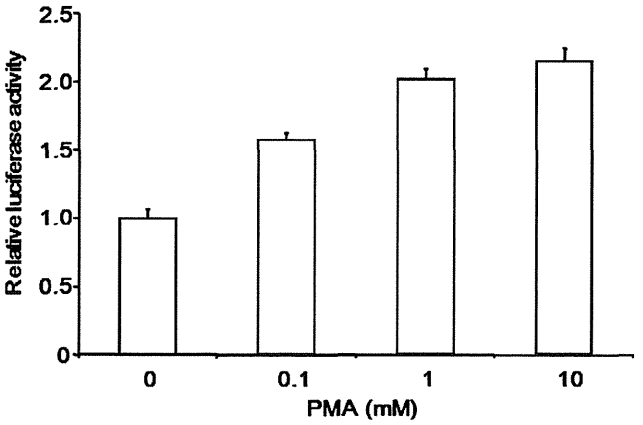


**Fig. 2.** Effect of PMA on the luciferase activity in clone 35 cells. Clone 35 cells were treated with PMA at the indicated concentrations for 24 h. Luciferase activity in the lysates was measured. The relative luciferase activity is shown as the ratio of the luciferase activity in the treated cells to that of the vehicle-treated cells. The data are means ± S.D. ($n = 3$). The results are representative of two independent experiments.

evaluate expression of the reporter gene, we checked the endogenous claudin-4 expression level in various cell lines and selected MCF-7, HaCat, HT1080, and SiHa cells, which have different claudin-4 expression levels for our analyses (Suppl. Fig. 1B). We transiently transfected the reporter plasmid into these cell lines and found that the luciferase activity of each was correlated with the endogenous expression level of claudin-4 (Suppl. Fig. 1C). We also investigated expression of the reporter gene in MCF-7 cells stably expressing snail or HRasV12, which suppress or induce claudin-4 expression, respectively [22,23]. Transfection of snail- or HRasV12-expressing MCF-7 cells with the reporter plasmid decreased or increased, respectively, the luciferase activity compared to that of mock-transfected MCF-7 cells (Fig. 1A and B). The difference in luciferase activity paralleled the level of claudin-4 mRNA in the cells (Fig. 1C and D), suggesting that the cloned promoter region was functional.

### 3.2. Preparation of a screening system for claudin-4 modulators

We transfected MCF-7 cells with the claudin-4 reporter plasmid and isolated stable transfected clones. We investigated the effect of transient expression of snail and HRasV12 on luciferase activity in these clones and found that several clones showed altered luciferase activity when transfected with the claudin-4 suppressor (snail, Suppl. Fig. 2A) or the claudin-4 inducer (HRasV12, Suppl. Fig. 2B). TGF-β suppresses claudin-4 expression [23], whereas EGF enhances claudin-4 expression [24]. Therefore, we also investigated the effects of TGF-β and EGF on the luciferase activity in the clones (Suppl. Fig. 2C and D, respectively). Since clone 35 showed the best

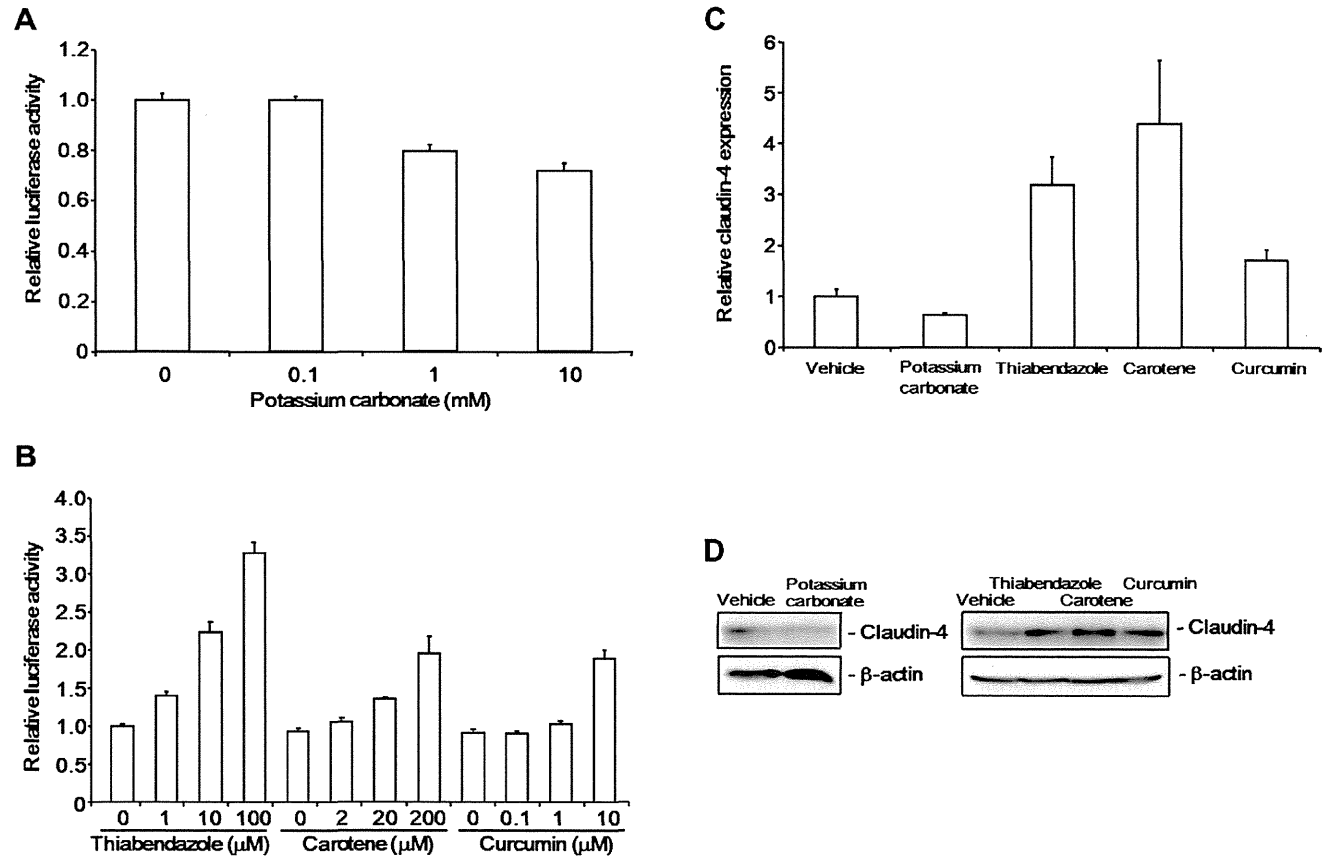


**Fig. 3.** Screening claudin-4 modulators using the reporter system. (A, B) Dose-dependent effects of the claudin-4 modulator candidates on luciferase expression. Clone 35 cells were treated with potassium carbonate (A), or thiabendazole, carotene, or curcumin (B) at the indicated concentrations for 24 h. Luciferase activity was measured in the lysates. Relative luciferase activity is shown as the ratio of the luciferase activity in the chemical-treated cells to that in the vehicle-treated cells. The data are means ± S.D. ($n = 3$). The results are representative of three independent experiments. (C, D) Effects of the claudin-4 modulator candidates on claudin-4 mRNA expression (C) and claudin-4 protein (D) levels. Clone 35 cells were treated with potassium carbonate (5 mM), thiabendazole (0.1 mM), carotene (0.2 mM), or curcumin (10 μM) for 24 h (C) or 48 h (D). Total RNA was used for qPCR analysis to detect claudin-4 mRNA (C). The relative mRNA expression of claudin-4 normalized to GAPDH expression. The cell lysates were subjected to SDS–PAGE, followed by immunoblotting for claudin-4 (D). GAPDH or β-actin served as loading controls. The result is representative of three independent experiments.

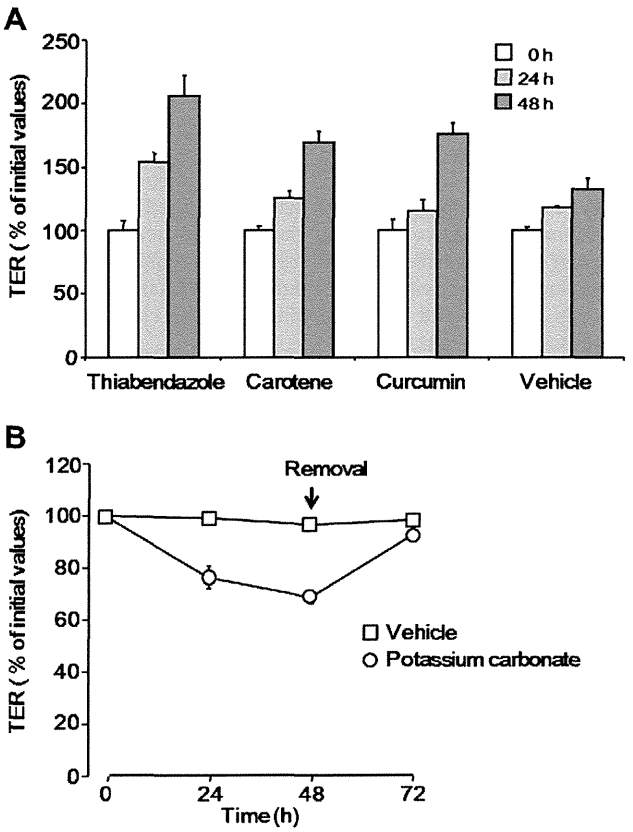


**Fig. 4.** Effects of claudin-4 modulator on the TJ-barrier in Caco-2 cells. (A) Effect of claudin-4 inducers on the TJ-barrier. Cells were seeded in Transwell™ chambers. Seven days after seeding, the cells were treated with thiabendazole (0.05 mM), carotene (0.2 mM), or curcumin (10 μM). TER values were monitored every 24 h. (B) Effect of a claudin-4 repressor on the TJ-barrier. Cells were seeded in Transwell™ chambers. When the TER values reached a plateau, the TJ-developed cells were treated with potassium carbonate (10 mM). After 48 h of treatment, the medium was replaced with fresh medium. The cells were then cultured for an additional 24 h. TER values were monitored every 24 h. TER values are shown as percentages of the TER values before treatment relative to those in treated cells, as described in the Section 2. The data are means ± S.D. ($n = 3$). These results are representative of three independent experiments.

response to the various claudin-4-modulating treatments, we selected it for further analysis. The clone 35 cells were treated with PMA, which enhances claudin-4 expression [25]. PMA increased luciferase activity in a dose-dependent manner (Fig. 2). These results indicate that clone 35 could be used to screen for modulators of claudin-4 expression.

### 3.3. Screening for claudin-4 modulators

When we eat, fragments of partially digested food, which still have antigenicity, exist in the intestine. This suggests that claudin modulators that tighten TJ-barriers may be contained in food. Therefore, we screened 86 chemicals used as food additives for claudin-4 modulators (Table 1). At first, we checked the cytotoxicity of these compounds in the clone 35 cells (Table 1). Then, we treated the cells with the compounds at non-toxic concentrations and identified the following claudin-4 modulator candidates: potassium carbonate (No. 3), thiabendazole (No. 68), carotene (No. 83), and curcumin (No. 86) (Suppl. Fig. 3). Each chemical modulated luciferase activity in a dose-dependent manner (Fig. 3A and B). qPCR analysis revealed that thiabendazole, carotene, and curcumin increased claudin-4 expression in the clone 35 cells (Fig. 3C), whereas potassium carbonate decreased claudin-4 expression. Similar results were obtained from Western blot analysis of claudin-4 (Fig. 3D).

To test whether the screened compounds also modulated the TJ-barrier, we investigated the effect of the compounds on the TER value, a marker of TJ-integrity, in Caco-2 cell monolayers, which is a popular model for mucosal barrier. Treatment of cells with thiabendazole, carotene, and curcumin increased the TER values (Fig. 4A). In contrast, potassium carbonate decreased the TER value. Moreover, the TER values recovered when the potassium carbonate was removed (Fig. 4B), and treatment with potassium carbonate did not cause cytotoxicity (data not shown). Thus, we successfully identified claudin-4 modulators.

## 4. Discussion

Claudin-4 inducers have been the focus of attention in drug development to treat inflammatory diseases and cancers [17–19]; however, their development has been slow. Some chemicals that modulate TJ integrity have been identified: glutamine, bryostatin-1, berberine, quercetin, and butyrate [26–30]. Here, we established a simple monitoring system for claudin-4 expression using a reporter gene, luciferase, and successfully identified chemical claudin-4 modulators: one suppressor of claudin-4 expression, potassium carbonate, and three inducers of claudin-4, thiabendazole, carotene, and curcumin.

Curcumin is an active ingredient of the spice turmeric, which is used in curry powders and as a food preservative. It is also used in traditional medicine to treat various inflammatory conditions, such as arthritis, colitis, and hepatitis [31]. Curcumin has various biological activities, such as anti-inflammatory, anti-oxidant, and anti-cancer effects [32]; however, the underlying mechanisms have never been fully understood. Here, we found that curcumin induces claudin-4 expression and increases TJ integrity. This enhancement of TJ integrity by curcumin may be associated with its therapeutic activities.

Carotene is a precursor of vitamin A. Retinoic acid, a metabolite of vitamin A, enhances TJ integrity in epithelial cells accompanied by expression of claudin-1, -4, and occludin [33]. These findings suggest that metabolized β-carotene-activated expression of claudins enhances the epithelial barrier in Caco-2 cells. Retinoic acid is a biologically active regulator of cell differentiation, proliferation, and apoptosis in various cell types [34]. The activities of retinoic acid are mediated by two types of nuclear receptors: retinoic acid receptors and their heterodimeric counterparts, retinoid X receptors [35]. Specific heterodimer-mediated transcriptional activation increases TJ integrity [36]. The increase in claudin-4 expression and TJ integrity induced by carotene may be caused by the formation of the heterodimer, followed by transcriptional activation.

Thiabendazole is used as a broad spectrum anthelmintic in various animal species and is also used to control parasitic infections in humans [37]. It is also used as an anti-fungal agent for the treatment of fruits [38]. Here, we found that thiabendazole increases claudin-4 expression and TJ integrity, but the mechanism for these activities remains unclear.

Our screening system identified a repressor of intestinal epithelial barrier function as well as three enhancers. We showed that potassium carbonate reduces claudin-4 expression and epithelial barrier function in Caco-2 cells without causing cytotoxicity. Potassium carbonate is used as an acidity regulator, and paracellular permeability is sensitive to pH [39]. Thus, potassium carbonate might reduce epithelial barrier integrity by changing the pH.

In conclusion, we developed the simple screening system for claudin-4 modulator, and we identified several claudin-4 modulators, including three inducers and one repressor. The screening system will thus be a tool for the development of claudin-4

modulators, thereby contributing to basic and pharmaceutical researches.

## Acknowledgments

This work was supported by a Grant-in-Aid for Scientific Research from the Ministry of Education, Culture, Sports, Science, and Technology, Japan (21689006; 24390042), by a Health and Labor Sciences Research Grant from the Ministry of Health, Labor, and Welfare of Japan and by the Takeda Science Foundation.

## Appendix A. Supplementary data

Supplementary data associated with this article can be found, in the online version, at http://dx.doi.org/10.1016/j.bbrc.2012.08.083.

## References

[1] M. Cereijido, R.G. Contreras, L. Shoshani, D. Flores-Benitez, I. Larre, Tight junction and polarity interaction in the transporting epithelial phenotype, Biochim. Biophys. Acta 1778 (2008) 770–793.
[2] D.W. Powell, Barrier function of epithelia, Am. J. Physiol. 241 (1981) G275–288.
[3] A. Wodarz, I. Nathke, Cell polarity in development and cancer, Nat. Cell Biol. 9 (2007) 1016–1024.
[4] B.J. Aungst, Intestinal permeation enhancers, J. Pharm. Sci. 89 (2000) 429–442.
[5] M. Kondoh, T. Yoshida, H. Kakutani, K. Yagi, Targeting tight junction proteins-significance for drug development, Drug Discovery Today 13 (2008) 180–186.
[6] H. Chiba, M. Osanai, M. Murata, T. Kojima, N. Sawada, Transmembrane proteins of tight junctions, Biochim. Biophys. Acta 1778 (2008) 588–600.
[7] L.L. Mitic, V.M. Unger, J.M. Anderson, Expression, solubilization, and biochemical characterization of the tight junction transmembrane protein claudin-4, Protein Sci. 12 (2003) 218–227.
[8] M. Furuse, S. Tsukita, Claudins in occluding junctions of humans and flies, Trends Cell Biol. 16 (2006) 181–188.
[9] K. Morita, M. Furuse, K. Fujimoto, S. Tsukita, Claudin multigene family encoding four-transmembrane domain protein components of tight junction strands, Proc. Natl. Acad. Sci. USA 96 (1999) 511–516.
[10] M. Furuse, M. Hata, K. Furuse, Y. Yoshida, A. Haratake, Y. Sugitani, T. Noda, A. Kubo, S. Tsukita, Claudin-based tight junctions are crucial for the mammalian epidermal barrier: a lesson from claudin-1-deficient mice, J. Cell Biol. 156 (2002) 1099–1111.
[11] A. Gow, C.M. Southwood, J.S. Li, M. Pariali, G.P. Riordan, S.E. Brodie, J. Danias, J.M. Bronstein, B. Kachar, R.A. Lazzarini, CNS myelin and sertoli cell tight junction strands are absent in Osp/claudin-11 null mice, Cell 99 (1999) 649–659.
[12] T. Nitta, M. Hata, S. Gotoh, Y. Seo, H. Sasaki, N. Hashimoto, M. Furuse, S. Tsukita, Size-selective loosening of the blood–brain barrier in claudin-5-deficient mice, J. Cell Biol. 161 (2003) 653–660.
[13] P.J. Morin, Claudin proteins in human cancer: promising new targets for diagnosis and therapy, Cancer Res. 65 (2005) 9603–9606.
[14] J.D. Schulzke, S. Ploeger, M. Amasheh, A. Fromm, S. Zeissig, H. Troeger, J. Richter, C. Bojarski, M. Schumann, M. Fromm, Epithelial tight junctions in intestinal inflammation, Ann. N. Y. Acad. Sci. 1165 (2009) 294–300.
[15] N. Sonoda, M. Furuse, H. Sasaki, S. Yonemura, J. Katahira, Y. Horiguchi, S. Tsukita, *Clostridium perfringens* enterotoxin fragment removes specific claudins from tight junction strands: evidence for direct involvement of claudins in tight junction barrier, J. Cell Biol. 147 (1999) 195–204.
[16] H. Uchida, M. Kondoh, T. Hanada, A. Takahashi, T. Hamakubo, K. Yagi, A claudin-4 modulator enhances the mucosal absorption of a biologically active peptide, Biochem. Pharmacol. 79 (2010) 1437–1444.
[17] R. Mennigen, K. Nolte, E. Rijcken, M. Utech, B. Loeffler, N. Senninger, M. Bruewer, Probiotic mixture VSL#3 protects the epithelial barrier by maintaining tight junction protein expression and preventing apoptosis in a murine model of colitis, Am. J. Physiol. 296 (2009) G1140–1149.
[18] S.K. Lee, J. Moon, S.W. Park, S.Y. Song, J.B. Chung, J.K. Kang, Loss of the tight junction protein claudin 4 correlates with histological growth-pattern and differentiation in advanced gastric adenocarcinoma, Oncol. Rep. 13 (2005) 193–199.
[19] S. Mima, S. Tsutsumi, H. Ushijima, M. Takeda, I. Fukuda, K. Yokomizo, K. Suzuki, K. Sano, T. Nakanishi, W. Tomisato, T. Tsuchiya, T. Mizushima, Induction of claudin-4 by nonsteroidal anti-inflammatory drugs and its contribution to their chemopreventive effect, Cancer Res. 65 (2005) 1868–1876.
[20] H. Honda, M.J. Pazin, H. Ji, R.P. Wernyj, P.J. Morin, Crucial roles of Sp1 and epigenetic modifications in the regulation of the CLDN4 promoter in ovarian cancer cells, J. Biol. Chem. 281 (2006) 21433–21444.
[21] T. Vincent, E.P. Neve, J.R. Johnson, A. Kukalev, F. Rojo, J. Albanell, K. Pietras, I. Virtanen, L. Philipson, P.L. Leopold, R.G. Crystal, A.G. de Herreros, A. Moustakas, R.F. Pettersson, J. Fuxe, A SNAIL1-SMAD3/4 transcriptional repressor complex promotes TGF-beta mediated epithelial–mesenchymal transition, Nat. Cell Biol. 11 (2009) 943–950.
[22] J. Ikenouchi, M. Matsuda, M. Furuse, S. Tsukita, Regulation of tight junctions during the epithelium–mesenchyme transition: direct repression of the gene expression of claudins/occludin by snail, J. Cell Sci. 116 (2003) 1959–1967.
[23] P. Michl, C. Barth, M. Buchholz, M.M. Lerch, M. Rolke, K.H. Holzmann, A. Menke, H. Fensterer, K. Giehl, M. Lohr, G. Leder, T. Iwamura, G. Adler, T.M. Gress, Claudin-4 expression decreases invasiveness and metastatic potential of pancreatic cancer, Cancer Res. 63 (2003) 6265–6271.
[24] A. Ikari, K. Atomi, A. Takiguchi, Y. Yamazaki, M. Miwa, J. Sugatani, Epidermal growth factor increases claudin-4 expression mediated by Sp1 elevation in MDCK cells, Biochem. Biophys. Res. Commun. 384 (2009) 306–310.
[25] C. Wray, Y. Mao, J. Pan, A. Chandrasena, F. Piasta, J.A. Frank, Claudin-4 augments alveolar epithelial barrier function and is induced in acute lung injury, Am. J. Physiol. 297 (2009) L219–227.
[26] L. Gu, N. Li, Q. Li, Q. Zhang, C. Wang, W. Zhu, J. Li, The effect of berberine in vitro on tight junctions in human Caco-2 intestinal epithelial cells, Fitoterapia 80 (2009) 241–248.
[27] N. Li, V.G. DeMarco, C.M. West, J. Neu, Glutamine supports recovery from loss of transepithelial resistance and increase of permeability induced by media change in Caco-2 cells, J. Nutr. Biochem. 14 (2003) 401–408.
[28] L. Peng, Z.R. Li, R.S. Green, I.R. Holzman, J. Lin, Butyrate enhances the intestinal barrier by facilitating tight junction assembly via activation of AMP-activated protein kinase in Caco-2 cell monolayers, J. Nutr. 139 (2009) 1619–1625.
[29] T. Suzuki, H. Hara, Quercetin enhances intestinal barrier function through the assembly of zonula [corrected] occludens-2, occludin, and claudin-1 and the expression of claudin-4 in Caco-2 cells, J. Nutr. 139 (2009) 965–974.
[30] J. Yoo, A. Nichols, J.C. Song, J. Mammen, I. Calvo, R.T. Worrell, J. Cuppoletti, K. Matlin, J.B. Matthews, Bryostatin-1 attenuates TNF-induced epithelial barrier dysfunction: role of novel PKC isozymes, Am. J. Physiol. 284 (2003) G703–712.
[31] J. Epstein, I.R. Sanderson, T.T. Macdonald, Curcumin as a therapeutic agent: the evidence from in vitro, animal and human studies, Br. J. Nutr. 103 (2010) 1545–1557.
[32] R.K. Maheshwari, A.K. Singh, J. Gaddipati, R.C. Srimal, Multiple biological activities of curcumin: a short review, Life Sci. 78 (2006) 2081–2087.
[33] M. Osanai, N. Nishikiori, M. Murata, H. Chiba, T. Kojima, N. Sawada, Cellular retinoic acid bioavailability determines epithelial integrity: role of retinoic acid receptor alpha agonists in colitis, Mol. Pharmacol. 71 (2007) 250–258.
[34] M. Osanai, M. Petkovich, Expression of the retinoic acid-metabolizing enzyme CYP26A1 limits programmed cell death, Mol. Pharmacol. 67 (2005) 1808–1817.
[35] P. Kastner, M. Mark, P. Chambon, Nonsteroid nuclear receptors: what are genetic studies telling us about their role in real life?, Cell 83 (1995) 859–869
[36] H. Kubota, H. Chiba, Y. Takakuwa, M. Osanai, H. Tobioka, G. Kohama, M. Mori, N. Sawada, Retinoid X receptor alpha and retinoic acid receptor gamma mediate expression of genes encoding tight-junction proteins and barrier function in F9 cells during visceral endodermal differentiation, Exp. Cell Res. 263 (2001) 163–172.
[37] K. Walton, R. Walker, J.J. van de Sandt, J.V. Castell, A.G. Knapp, G. Kozianowski, M. Roberfroid, B. Schilter, The application of in vitro data in the derivation of the acceptable daily intake of food additives, Food Chem. Toxicol. 37 (1999) 1175–1197.
[38] J.P. Groten, W. Butler, V.J. Feron, G. Kozianowski, A.G. Renwick, R. Walker, An analysis of the possibility for health implications of joint actions and interactions between food additives, Regul. Toxicol. Pharmacol. 31 (2000) 77–91.
[39] V.W. Tang, D.A. Goodenough, Paracellular ion channel at the tight junction, Biophys. J. 84 (2003) 1660–1673.

molecular pharmaceutics

Brief Article

pubs.acs.org/molecularpharmaceutics

# Involvement of $Ca^{2+}$ and ATP in Enhanced Gene Delivery by Bubble Liposomes and Ultrasound Exposure

Daiki Omata,[†] Yoichi Negishi,*[,†] Sho Yamamura,[†] Shoko Hagiwara,[†] Yoko Endo-Takahashi,[†] Ryo Suzuki,[‡] Kazuo Maruyama,[‡] Motoyoshi Nomizu,[§] and Yukihiko Aramaki[†]

[†]Department of Drug Delivery and Molecular Biopharmaceutics, School of Pharmacy, Tokyo University of Pharmacy and Life Sciences, Hachioji, Tokyo 192-0392, Japan

[‡]Department of Biopharmaceutics, School of Pharmaceutical Sciences, Teikyo University, Sagamihara, Kanagawa 252-5195, Japan

[§]Department of Clinical Biochemistry, School of Pharmacy, Tokyo University of Pharmacy and Life Sciences, Hachioji, Tokyo 192-0392, Japan

**ABSTRACT:** Recently, we reported the accelerated gene transfection efficiency of laminin-derived AG73-peptide-labeled polyethylene glycol-modified liposomes (AG73-PEG liposomes) and cell penetrating TAT-peptide labeled PEG liposomes using PEG-modified liposomes, which trap echo-contrast gas, "Bubble liposomes" (BLs), and ultrasound (US) exposure. BLs and US exposure were reported to enhance the endosomal escape of AG73-PEG liposomes, thereby leading to increased gene expression. However, the mechanism behind the effect of BLs and US exposure on endosomes is not well understood. US exposure was reported to induce an influx of calcium ions ($Ca^{2+}$) by enhancing permeability of the cell membrane. Therefore, we examined the effect of $Ca^{2+}$ on the endosomal escape and transfection efficiency of AG73-PEG liposomes, which were previously enhanced by BLs and US exposure. For cells treated with EGTA, the endosomal escape and gene expression of AG73-PEG liposomes were not enhanced by BLs and US exposure. Similarly, transfection efficiency of the AG73-PEG liposomes in ATP-depleted cells was not enhanced. Our results suggest that $Ca^{2+}$ and ATP are necessary for the enhanced endosomal escape and gene expression of AG73-PEG liposomes by BLs and US exposure. These findings may contribute to the development of useful techniques to improve endosomal escape and achieve efficient gene transfection.

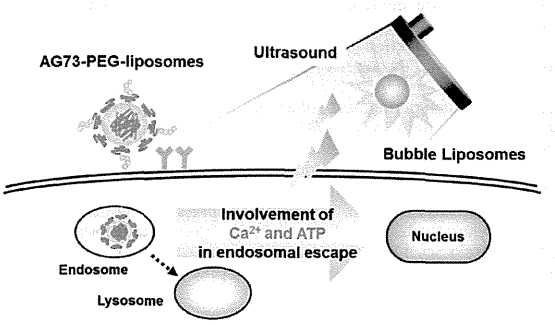


**KEYWORDS:** *AG73 peptide, atp, Bubble liposomes, calcium ions, gene delivery, endosomal escape, ultrasound*

## ■ INTRODUCTION

For successful gene therapy, various nonviral vectors such as lipid- and polymer-based carriers have been developed. However, they generally have relatively low transfection efficiencies, which need to be overcome.[1] Recent reports have emphasized the importance of subcellular and intracellular trafficking of gene delivery carriers. To achieve efficient gene transfection, carriers must overcome several steps including cellular internalization, endosomal escape, nuclear transfer and intracellular transcription.[2,3] Of these steps, endosomal escape is considered one of the most important, because most carriers are internalized into cells via an endocytic pathway. When escape from endosomes is impossible, the genes are degraded in lysosomes. Indeed, some groups have developed carriers and protocols that involve monitoring functions, such as pH sensitivity, temperature dependence, or photosensitivity, to deliver genes to the cytosol from endosomes.[4−7]

Previously, we developed laminin-derived AG73 peptide-labeled polyethylene glycol (PEG)-modified liposomes (AG73-PEG liposomes) as tumor targeted gene delivery carriers.[8] We also reported that the transfection efficiency of AG73-PEG liposomes and TAT-PEG liposomes, which were labeled with a TAT peptide (a cell penetrating peptide derived from human immunodeficiency virus trans-acting transcriptional activator), could be accelerated by PEG-modified liposomes, which trap echo-contrast gas, "Bubble liposomes" (BLs), and ultrasound (US) exposure.[9,10] BLs and US exposure enhanced the endosomal escape of AG73-PEG liposomes and TAT-PEG liposomes, leading to increased gene expression. However, the mechanism behind the effect of BLs and US exposure on endosomes and the resulting enhanced endosomal escape of carriers is not well understood. To promote this method as a more useful gene delivery tool, it is necessary to understand the detailed interactions at a fundamental level.

US pressure above a certain threshold can cause oscillating bubbles to undergo a violent collapse known as inertial cavitation. Microbubbles can be the nuclei of cavitation, and

**Received:** November 28, 2011
**Revised:** January 26, 2012
**Accepted:** March 2, 2012
**Published:** March 2, 2012

ACS Publications © 2012 American Chemical Society

subsequent US exposure can induce more efficient cavitation. Inertial cavitation is thought to cause transient disruptions in cell membranes, which enable the transport of extracellular molecules into cells.[11−16] However, US exposure has also induced several biological effects, such as bone fracture healing, wound healing, and induction of apoptosis.[17−19] Moreover, the induced influx of calcium ions, the generation of reactive oxygen species, or the activation of some signals at a cellular level can be attributed to US exposure.[20−23]

Calcium ions ($Ca^{2+}$) have important roles in cells and are involved in various events such as cell proliferation and cell death.[24,25] US exposure induces the influx of $Ca^{2+}$ by enhancing permeability of the cell membrane. $Ca^{2+}$ also adjusts endosomal acidification and vesicle fusion.[26−29] Therefore, we focused on $Ca^{2+}$ and hypothesized that BLs and US enhance the endosomal escape of gene delivery carriers via $Ca^{2+}$ influx. We also investigated the involvement of ATP in enhanced gene delivery. In this study, we examined the effect of $Ca^{2+}$ and ATP on the endosomal escape and transfection efficiency of AG73-PEG liposomes enhanced by BLs and US exposure.

## ■ EXPERIMENTAL SECTION

**Materials.** The pcDNA3-Luc plasmid, derived from pGL3-basic (Promega, Madison, WI), is an expression vector encoding the firefly luciferase gene under the control of a cytomegalovirus promoter. EGTA (ethylene glycol-bis(2-aminoethyl ether)-*N,N,N′,N′*-tetraacetic acid) was purchased from Sigma (St. Louis, MO). NaF and $NaN_3$ were purchased from Wako Pure Chemical Industries, Ltd. (Osaka, Japan). Antimycin A was purchased from Enzo Life Sciences, Inc. . (Farmingdale, NY). Alexa Fluor 488-conjugated transferrin was purchased from Molecular Probes, Inc. (Eugene, OR).

**Cell Lines and Cultures.** A 293T human embryonic kidney carcinoma cell line, stably overexpressing syndecan-2 (293T-Syn2 cell), was cultured in Dulbecco's modified Eagle's medium (DMEM; Kohjin Bio Co. Ltd., Tokyo, Japan), supplemented with 10% fetal bovine serum (FBS; Equitech Bio Inc., Kerrville, TX), penicillin (100 U/mL), streptomycin (100 μg/mL), and puromycin (0.4 μg/mL), at 37 °C in humidified 5% $CO_2$ atmosphere.

**Preparation of AG73-PEG Liposomes.** The Cys-AG73 peptide (CGG-RKRLQVQLSIRT) was synthesized manually using the 9-fluorenylmethoxycarbony (Fmoc)-based solid-phase strategy. The peptide was prepared in the COOH-terminal amide form and purified by reverse phase high-performance liquid chromatography. AG73-labeled PEG liposomes were prepared by the hydration method. The pDNA was diluted to a concentration of 0.1 mg/mL in 10 mM HEPES buffer (pH 7.4) and was condensed using 0.1 mg/mL poly-L-lysine (PLL); (SIGMA-Aldrich Co., St. Louis, MO). The complex of pDNA-PLL was added to a lipid film composed of 1,2-dioleoyl-*sn*-glycero-3-phospho-*rac*-1-glycerol (DOPG) (AVANTI Polar Lipids Inc., Alabaster, AL), 1,2-dioleoyl-*sn*-glycero-3-phosphoethanolamine (DOPE) (AVANTI Polar Lipids Inc., Alabaster, AL), and 1,2-distearoyl-*sn*-glycero-3-phosphatidylethanolamine-polyethylene glycol-maleimide ($DSPE\text{-}PEG_{2000}$-Mal) (NOF Corporation, Tokyo, Japan) in a molar ratio of 2:9:0.57 followed by incubation for 10 min at room temperature to hydrate the lipids. The solution was sonicated for 5 min in a bath-type sonicator (42 kHz, 100 W) (BRANSONIC 2510J-DTH, Bransoni Ultrasonic Co., Danbury, CT). For coupling, AG73 peptide, at a molar ratio of 5-fold $DSPE\text{-}PEG_{2000}$-Mal, was added to the PEG liposomes, and the mixture was incubated for 6 h at room temperature to conjugate the cysteine of Cys-AG73 peptide to the maleimide of the PEG liposomes using a thioether bond. The resulting AG73-peptide-conjugated PEG liposomes (AG73-PEG liposomes) were dialyzed to remove any excess peptide. AG73-PEG liposomes were modified with 5 mol % PEG and 3 mol % peptides.

**Preparation of Bubble Liposomes.** PEG liposomes composed of 1,2-dipalmitoyl-*sn*-glycero-3-phosphocholine (DPPC) (NOF Corporation, Tokyo, Japan) and 1,2-distearoyl-*sn*-glycero-3-phosphatidylethanolamine-polyethylene glycol ($DSPE\text{-}PEG_{2000}$-OMe) (NOF Corporation, Tokyo, Japan) in a molar ratio of 94:6 were prepared by a reverse-phase evaporation method. In brief, all reagents were dissolved in 1:1 (v/v) chloroform/diisopropyl ether. Phosphate buffered saline was added to the lipid solution, and the mixture was sonicated and then evaporated at 47 °C. The organic solvent was completely removed, and the size of the liposomes was adjusted to less than 200 nm using extruding equipment and a sizing filter (pore size: 200 nm) (Nuclepore Track-Etched Membrane, GE Healthcare, U.K.). The lipid concentration was measured using a Phospholipid C test Wako (Wako Pure Chemical Industries, Ltd., Osaka, Japan). BLs were prepared from liposomes using perfluoropropane gas (Takachio Chemical Ind. Co. Ltd., Tokyo, Japan). First, 2 mL sterilized vials containing 0.8 mL of the liposome suspension (lipid concentration: 1 mg/mL) were filled with perfluoropropane gas, capped, and then pressurized with a further 3 mL of perfluoropropane gas. The vials were placed in a bath-type sonicator (42 kHz, 100 W) (BRANSONIC 2510j-DTH, Branson Ultrasonics Co., Danbury, CT) for 5 min to form BLs.

**Gene Transfection by AG73-PEG Liposomes with BLs and US Exposure.** Two days before the experiments, 293T-Syn2 cells ($1 \times 10^5$) were seeded in a 48-well plate. The cells were treated with AG73-PEG liposomes (encapsulating pDNA: 3 μg/mL) in serum-free medium for 4 h at 37 °C. The cells were washed twice with $Ca^{2+}$-free DMEM containing 10 mM EGTA. To deplete ATP, the cells were treated with $NaN_3$ (0.1%), NaF (10 mM), and antimycin A (1 μg/mL) for 30 min, and then the BLs were added. Within 2 min, US exposure was applied through a 6 mm diameter probe placed in the well (frequency, 2 MHz; duty, 50%; burst rate, 2 Hz; intensity, 1.0 $W/cm^2$; time, 10 s). A Sonopore 3000 (NEPA GENE, CO., Ltd., Chiba, Japan) was used to generate the US. The cells were transferred to fresh medium and cultured for 20 h, and then luciferase activity was determined.

**Measurement of Luciferase Expression.** Cell lysates were prepared with lysis buffer (0.1 M Tris-HCl pH 7.8, 0.1% Triton X-100, and 2 mM EDTA). Luciferase activity was measured as relative light units (RLU) per mg of protein using a luciferase assay system (Promega, Madison, WI) and a luminometer (LB96 V, Belthold Japan Co. Ltd., Tokyo, Japan).

**Assessment of Localization of pDNA and Transferrin.** The 293T-Syn2 cells ($7 \times 10^4$) were seeded two days before the experiments. The cells were treated with AG73-PEG liposomes (Cy3-labeled pDNA: 3 μg/mL) and Alexa Fluor 488-conjugated transferrin (50 μg/mL) for 4 h at 37 °C. After incubation, the cells were washed, and the BLs (120 μg/mL) were added. Then, US exposure was applied (frequency, 2028 kHz; duty, 50%; burst rate, 2.0 Hz; intensity, 1.0 $W/cm^2$; time, 10 s). To assess the involvement of $Ca^{2+}$ and ATP, the cells were treated as described in the above section. Subsequently, the cells were incubated for 10 min and then fixed with 4%

paraformaldehyde for 1 h at 4 °C followed by visualization using confocal laser scanning microscopy (CLSM). To differentiate the AG73-PEG liposomes internalized into the cytoplasm following attachment to the surface of the cell membrane, the cytoplasm was distinguished from the cell membrane as shown previously.[9,10,30,31] The rate of colocalization of Cy3-labeled pDNA with Alexa Fluor 488-conjugated transferrin was quantified as follows: amount of colocalization (%) = Cy3 $pixels_{colocalization}$/Cy3 $pixels_{total}$ × 100, where Cy3 $pixels_{colocalization}$ represents the number of Cy3 pixels colocalizing with Alexa Fluor 488-conjugated transferrin and Cy3 $pixels_{total}$ represents the total number of Cy3 pixels.

**Assessment of Localization of pDNA and lamp-2.** The 293T-Syn2 cells were first treated with AG73-PEG liposomes (Cy3-lableled pDNA: 3 μg/mL) for 4 h at 37 °C and then with BLs and US exposure. To assess the involvement of $Ca^{2+}$ and ATP, cells were treated as described in the above section. Subsequently, the cells were incubated for 1 h and then fixed with 4% paraformaldehyde for 1 h at 4 °C. The cells were washed with PBS and permeabilized for 5 min in 0.2% saponin, followed by treatment with 10% goat serum in PBS. Finally, the cells were incubated with anti-lamp2 Ab (Santa Cruz Biotechnology, Inc., Santa Cruz, CA) overnight at 4 °C and treated with Alexa Fluor 488-conjugated secondary Ab (Invitrogen Co., Carlsbad, CA) for 1 h at room temperature in the dark. Then, CLSM and analysis was performed as described in the above section.

## ■ RESULTS AND DISCUSSION

In previous reports, we have showed that BLs and US exposure could enhance endosomal escape and gene transfection of AG73-PEG liposomes. We have proposed the mechanism that the cavitation induced in the outside of cells by US exposure and BLs could affect endosomes, and then AG73-PEG liposomes internalized by endocytosis escaped from endosomes, leading to enhanced gene expression. It have been also confirmed that AG73-PEG liposomes could not be introduced into cytoplasm directly through the cell membrane after the US-mediated disruption of BLs. However, the exact mechanism of accelerated endosomal escape of carriers was not clear. US exposure induces the influx of $Ca^{2+}$ by enhancing permeability of the cell membrane.[21] In addition, $Ca^{2+}$ adjusts endosomal acidification and vesicle fusion.[26−29] Therefore, to evaluate the mechanism by which BLs and US exposure could promote the endosomal escape of AG73-PEG liposomes, we examined the effect of $Ca^{2+}$ on the endosomal escape and transfection efficiency of AG73-PEG liposomes enhanced by BLs and US exposure. ATP is involved in various reactions, such as acidification of endosomes, intracellular trafficking of vesicles and fusion of vesicles.[26] We also investigated the involvement of ATP-dependent processes in enhanced gene delivery.

First, to evaluate the involvement of $Ca^{2+}$ and ATP in gene expression enhanced by BLs and US exposure, we examined the effect of $Ca^{2+}$ and ATP on gene expression efficiency of AG73-PEG liposomes using 293T-Syn2 cells. The cells were incubated with AG73-PEG liposomes containing pcDNA3-Luc, and then treated with BLs and US exposure. After 20 h incubation, luciferase activity was assayed. BLs and US exposure enhanced the luciferase activity of AG73-PEG liposomes by approximately 60-fold compared to that of AG73-PEG liposomes alone.[9] By contrast, when the cells were treated with 10 mM EGTA before the treatment of BLs and US exposure, the enhancement ratio of luciferase activity by BLs and US exposure was decreased. To examine the effect of ATP on gene transfection efficiency, the cells were treated with $NaN_3$, NaF, and antimycin A to deplete ATP. The subsequent luciferase assay showed insignificant enhancement by BLs and US exposure. Conversely, when cells were treated with AG73-PEG liposomes alone, luciferase activity was not affected by $Ca^{2+}$ and ATP depletion (Figure 1). These results suggest that

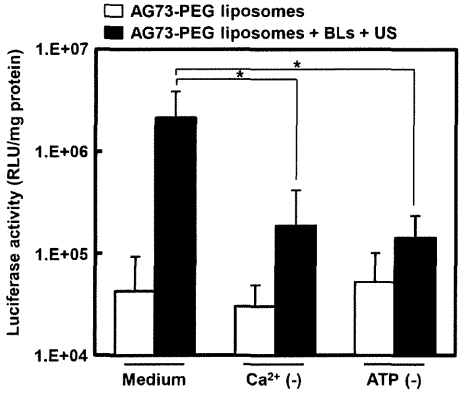


**Figure 1.** Effects of $Ca^{2+}$ and ATP on gene expression by AG73-PEG liposomes with BLs and US exposure. 293T-Syn2 cells were treated with AG73-PEG liposomes for 4 h at 37 °C, and then cells were washed twice with $Ca^{2+}$-free DMEM containing 10 mM EGTA for a depleted $Ca^{2+}$ condition. ATP was depleted by pretreating cells for 30 min before US exposure with 1 μg/mL antimycin A, 10 mM NaF, and 0.1% $NaN_3$. BLs (120 μg/mL) were added to cells followed by immediate US exposure. After replacement with fresh medium, the cells were cultured for 20 h and luciferase activity was determined. The data are shown as the means ± SD ($n$ = 4). *$p$ < 0.05.

$Ca^{2+}$ and ATP may be necessary to enhance gene transfection efficiency of AG73-PEG liposomes by BLs and US exposure. On the other hand, it is reported that extracellular $Ca^{2+}$ plays important roles to repair the cell membrane disruption and maintain cell survival.[32] Therefore, we examined the cell viability in $Ca^{2+}$-depleted condition. As a result, in this condition, the cell viability had almost no difference in the treatment with or without BLs and US exposure (data not shown). This result suggested that the decreased enhancement ratio of luciferase activity by the treatment of BLs and US exposure in $Ca^{2+}$-depleted condition was not due to a change of cell viability.

Recent reports have emphasized the importance of subcellular and intracellular trafficking of gene delivery carriers.[2,3] Among the several steps involeved, endosomal escape is considered one of the most important. In previous study, we have reported that enhanced endosomal escape of AG73-PEG liposomes by BLs and US exposure could increase gene expression.[9] Therefore, we evaluated the involvement of $Ca^{2+}$ and ATP on the endosomal escape of gene delivery carriers. We examined the effects of $Ca^{2+}$ and ATP on localization of pDNA encapsulated in AG73-PEG liposomes and transferrin, as an endosome marker,[33] by confocal microscopy. BLs and US exposure enhanced the endosomal escape of AG73-PEG liposomes and decreased the ratio of colocalization of pDNA and transferrin.[9] The 293T-Syn2 cells were first incubated with AG73-PEG liposomes containing Cy3-labeled pDNA and Alexa Fluor 488-conjugated transferrin and then treated with BLs and US exposure. The cells were observed by confocal microscopy to assess the colocalization of

Cy3-labeled pDNA and Alexa Fluor 488-conjugated transferrin. As shown in Figure 2a, the pDNA internalized into cells were

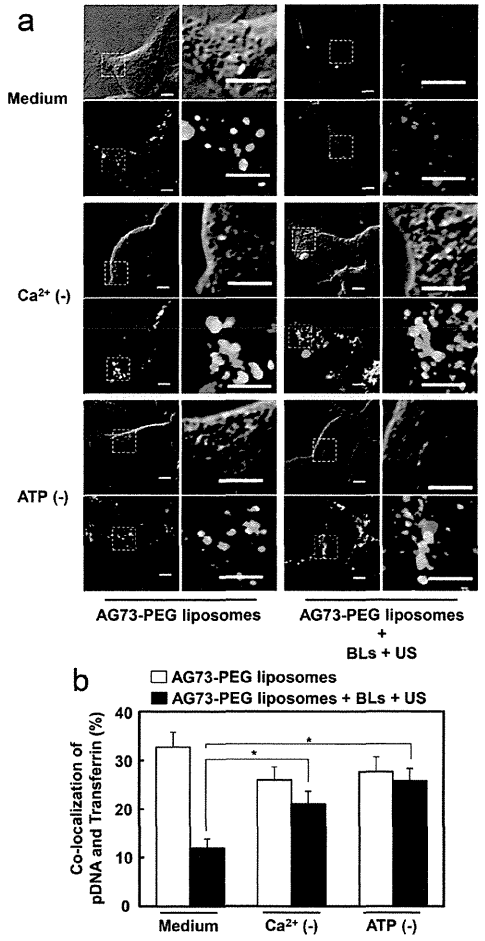


**Figure 2.** Effects of $Ca^{2+}$ and ATP on intracellular localization of pDNA and endosomes. (a, b) The 293T-Syn2 cells were treated with AG73-PEG liposomes encapsulating Cy3-labeled pDNA (red) and Alexa Fluor 488-conjugated transferrin (green) for 4 h at 37 °C and then washed twice with $Ca^{2+}$-free DMEM containing 10 mM EGTA to create $Ca^{2+}$-depleted conditions. ATP was depleted by pretreating cells for 30 min before US exposure with 1 μg/mL antimycin A, 10 mM NaF, and 0.1% $NaN_3$. BLs (120 μg/mL) were added to cells followed by immediate US exposure. The cells were incubated for 10 min, fixed with 4% paraformaldehyde for 1 h at 4 °C and observed by CLSM. The areas within the dotted square are shown as enlarged images. The scale bars represent 5 μm. The ratio of colocalization of Cy3-labeled pDNA with Alexa Fluor 488-conjugated transferrin was quantified. The data are shown as means ± SE ($n$ = 50). *$p$ < 0.05 compared with AG73-PEG liposomes alone (Mann–Whitney's $U$ test).

colocalized with transferrin, whereas BLs and US exposure decreased the colocalization of the pDNA and transferrin. However, when cells were treated with 10 mM EGTA, BLs and US exposure did not affect the intracellular localization of the pDNA and transferrin. In the ATP-depleted state, BLs and US exposure had no effect on the intracellular localization of the pDNA and transferrin. Furthermore, we calculated the ratio of colocalization of the pDNA and transferrin and found that BLs and US exposure decreased the ratio of colocalization. By contrast, when cells were treated with 10 mM EGTA or were exposed in an ATP-depleted state, BLs and US exposure did not affect the ratio of colocalization of pDNA and transferrin (Figure 2b). These results suggest that $Ca^{2+}$ and ATP may be required for endosomal escape of AG73-PEG liposomes after the addition of BLs and US exposure.

Efficient gene transfection requires sufficient delivery of genes from the endosomes to the cytosol, to avoid the degradation of genes in lysosomes. Therefore, we assessed the intracellular localization of pDNA and lysosomes and the effects of $Ca^{2+}$ and ATP on localization of pDNA and lysosomes. The 293T-Syn2 cells were treated with AG73-PEG liposomes containing Cy3-labeled pDNA, followed by the addition of BLs and application of US. The cells were fixed and stained with antibodies for lamp-2, a lysosome marker.[34] As a result, the pDNA internalized into cells was colocalized with lamp-2 at 10 or 60 min, whereas BLs and US exposure decreased the colocalization of pDNA and lamp-2 at 60 min after US exposure (Figure3). Moreover, when cells were treated with 10 mM EGTA and depleted of ATP, BLs and US exposure did not decrease the localization of pDNA and lamp-2 (Figure

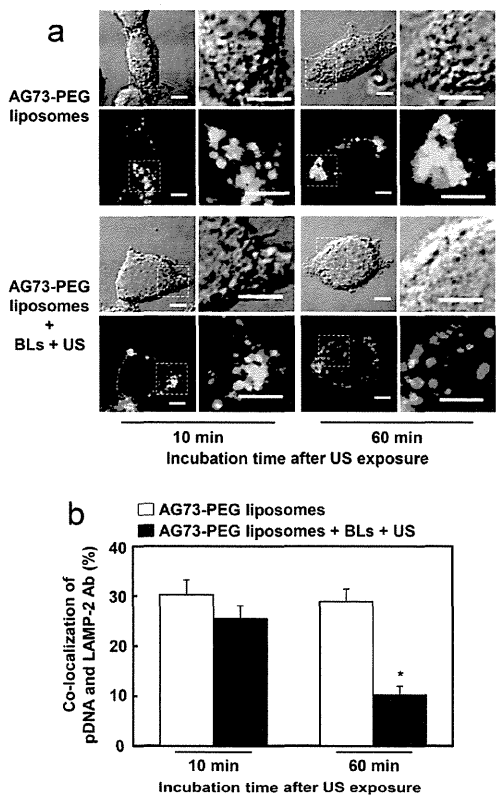


**Figure 3.** Effect of BLs and US exposure on intracellular localization of pDNA and lysosomes. The 293T-Syn2 cells were treated with AG73-PEG liposomes encapsulating Cy3-labeled pDNA (red) for 4 h at 37 °C. BLs (120 μg/mL) were added to cells followed by immediate US exposure. The cells were incubated for 10 or 60 min and then fixed with 4% paraformaldehyde for 1 h at 4 °C followed by staining with antibodies for lamp-2 (green), a marker for lysosomes. The cells were observed by CLSM. The areas within the dotted square are shown as enlarged images. The scale bars represent 5 μm. The ratio of colocalization of Cy3-labeled pDNA with lamp-2 was quantified. The data are shown as means ± SE ($n$ = 50). *$p$ < 0.05 (Mann–Whitney's $U$ test).


dx.doi.org/10.1021/mp200606d | Mol. Pharmaceutics 2012, 9, 1017–1023